viral RNA in 3D-cultured RCYM1 cells compared to that in monolayer cultures containing similar cell numbers. The doubling time of cells grown in TGP or RFB culture was approximately twice that observed in monolayer culture. Although it is possible that amino acid substitutions of culture-adaptive mutations contribute to interference with virus production, another possibility might be that in cases of certain HCV clones, higher expression of the viral proteins leads to their misfolding, thereby precluding the formation of virus particles.

Complete cell culture systems for HCV have recently been developed (Lindenbach et al., 2005; Wakita et al., 2005; Zhong et al., 2005) using a genotype 2a isolate, JFH-1, obtained from a Japanese patient with fulminant hepatitis (Date et al., 2004; Kato et al., 2001, 2003). Unlike many other HCV isolates, JFH-1-based subgenomic replicons do not require culture-adaptive mutations for efficient RNA replication (Kato et al., 2003). Transfection of Huh-7 cells with the full-length JFH-1 genome or a chimeric genome using JFH-1 and J6 results in the efficient production of infectious HCV (Lindenbach et al., 2005; Wakita et al., 2005; Zhong et al., 2005). This newly established HCV culture system is undoubtedly useful for a variety of HCV studies; however, these systems rely on the JFH-1 replicase (NS3 to 5B) and little is known about the reasons that this particular isolate permits efficient HCV production. Virus yield in the 3D systems presented here is significantly lower than that in systems based on JFH-1; it seems that 0.1–1 copies of HCV RNA/cell/day are generated and assembled into viral particles. The ratio of viral RNA to the core protein in these fractions is approximately 10^5 RNA copies/1 fmol of the core. Although only moderate production of HCV particles is observed in 3D culture of RCYM1 cells, this is the first study to demonstrate the production of infectious HCV particles derived from genotype 1b, which is highly prevalent worldwide and is thought to present a higher risk of developing hepatocellular carcinoma and/or cirrhosis than infections with other HCV types (Bruno et al., 1997; Silini et al., 1996). The findings of the present study may also suggest that an extremely high efficiency of viral replication, such as that observed in the case of JFH-1 isolate, is not needed to produce HCV particles in 3D cultures of Huh-7 cells. Heller et al. (2005) report HCV virion production in a culture transfected with the genomic cDNA of genotype 1b; however, the infectivity of the virus particles remains to be determined. More recently, it was shown that chimeric HCV containing structural proteins of genotypes 1a, 1b, or 3a was produced from fusion of the core to the p7 or NS2 region with downstream nonstructural regions of JFH1 clone, but that intergenotypic chimeras frequently yielded lower titers of infectious HCV compared to JFH1 or J6/JFH1 chimera (Pietschmann et al., personal communication). The 3D culture system described in the present study might be a helpful method of increasing the efficiency of assembly and release of intergenotypic chimeric HCV.

In summary, we found that the expression of dicistronic genome-length Con1 HCV RNA of genotype 1b in 3D-cultured Huh-7 cells yields infectious virus particles, and we demonstrated the usefulness for producing HCV particles of two 3D culture systems based on RFB and TGP, in which human hepatoma cells can assemble into spheroids with potentially polarized morphology. HCV morphogenesis occurs in a complex cellular environment in which host factors may either enhance or reduce the assembly and budding process. The culture system described here will allow us to further study viral morphogenesis and the biophysical properties of HCV particles, and it provides a new tool for the future development of anti-HCV drugs.

Materials and methods

Cell lines bearing dicistronic HCV RNAs

To generate a stable cell line harboring genome-length dicistronic HCV RNA, we electroporated 10^7 Huh-7 cells with 50 μg of the RNA transcribed from a plasmid pFKI389neo/core-3′/NK5.1 (Pietschmann et al., 2002). The cells were maintained in Dulbecco's modified Eagle's medium with 10% fetal bovine serum and 0.5 mg/ml G418 (Promega). After stringent selection for 3 weeks, a fast-growing clone was isolated and designated as RCYM1. A Huh-7-derived cell line, 5–15, harboring a subgenomic replicon (Lohmann et al., 1999) was also used.

3D cell cultures

The RFB system (Able, Japan) was manipulated as described previously (Aizaki et al., 2003) with minor modifications. Briefly, the RFB column, being filled with 4 ml of porous carrier beads made from polyvinyl alcohol, seeded with 1×10^7 of RCYM1 or 5–15 cells. The cells were cultured in ASF104 medium (Ajinomoto, Japan) supplemented with 4 g/l of D-glucose, 2% fetal calf serum, and 0.5 mg/ml of G418 (Promega). TGP (Mebiol Gel MB-10; Mebiol, Japan) was supplied as a lyophilized form and its aqueous solution was prepared before use as previously described (Hishikawa et al., 2004; Nagaya et al., 2004; Yoshioka et al., 1994). Briefly, TGP in a flask was dissolved in 10 ml of the culture medium and was maintained at 4 °C overnight. To prepare HCV particles, we suspended 5×10^6 cells of RCYM1 in 10 ml of TGP solution and aliquots were poured into a multi-well plate. Upon warming to 37 °C, the TGP solution quickly turned into a gel form, and 3 volumes of the culture medium were added to cover the gel. To recover spheroid cells and the culture supernatant after cultivation, we subjected the cultured plate to a temperature of 4 °C for 10 min to dissolve the gel. In order to separate spheroid cells from the culture medium, we subsequently centrifuged the TGP culture diluted with the overlaid culture medium at 1000×*g* for 5 min.

Sucrose density gradient centrifugation

The culture medium collected from the RFB or TGP was centrifuged at 8000 × *g* for 50 min to remove all cellular debris, after which the supernatant was centrifuged at 25,000 rpm at 4 °C for 4 h with an SW28 rotor (Beckman). The precipitant was suspended in 1 ml of TNE buffer [10 mM Tris–HCl (pH 7.8), 1 mM EDTA, 100 mM NaCl] and was then layered on top of continuous 10–60% (wt/vol) sucrose gradient in TNE buffer,

followed by centrifugation at 35,000 rpm at 4 °C for 14 h with an SW41E rotor (Beckman). Fractions (1 ml each) were collected from the top of the tube (12 fractions in total). The density of each fraction was determined by the weight of 100 μl of the fraction. For NP40 treatment, 0.5 ml of the TNE-suspended sample as described above was supplemented with 10 μl of RNase inhibitor (Takara, Japan) and 5 μl of 1M DTT, which was diluted by adding NP40 solution to a final concentration of 0.2%. After incubation at 4 °C for 20 min, the sample was fractionated by discontinuous 10–60% sucrose gradient centrifugation.

Quantitation of HCV RNA and core protein

Total RNA was extracted from cells and from the culture medium using TRIZOL (Invitrogen) and a QIAamp Viral RNA Mini spin column (Qiagen), respectively. Real-time RT-PCR was performed using TaqMan EZ RT-PCR Core Reagents (PE Applied Biosystems), as described previously (Aizaki et al., 2004; Suzuki et al., 2005). HCV core antigen within cells and culture medium was measured by immunoassay (Ortho HCV-Core ELISA Kit; Ortho-Clinical Diagnotics), following the manufacturer's instructions.

Western blot analysis

The protein concentration of cells recovered from monolayer or 3D cultures was determined by BCA Protein Assay Kit (Pierce). Aliquots of samples were analyzed by sodium dodecyl sulfate–polyacrylamide gel electrophoresis (SDS–PAGE) and transferred to polyvinylidene difluoride membranes (Immobilon; Millipore, Japan) using a semidry blotter. After overnight incubation at 4 °C in blocking buffer (Dainippon Pharmaceuticals, Japan) with 0.2% Tween 20, the membranes were incubated with appropriately diluted anti-HCV core (Anogen) and anti-NS5A (Austral Biologicals) monoclonal antibody, followed by incubation with horseradish peroxidase conjugated anti-mouse immunoglobulin G (Cell Signaling). The blots were then washed and developed with enhanced SuperSignal West Pico Chemiluminecent Substrate (Pierce).

Immunocytochemistry

For NS5A staining, infected cells cultured on collagen-coated coverslips were washed with phosphate buffered saline (PBS) and fixed with 4% paraformaldehyde at 4 °C for 30 min, followed by permeabilization with PBS containing 0.2% TritonX-100. After preincubation with BlockAce (Dainippon Pharmaceuticals), the samples were stained using mouse anti-NS5A antibody and rhodamine-conjugated goat anti-mouse IgG (ICN Pharmaceuticals) as the first and second antibodies, respectively.

Electron microscopy

To visualize HCV-LPs secreted into the medium, we concentrated and adsorbed sucrose density fractions prepared as described above onto carbon-coated grids for 1 min. The grids were stained with 1% uranyl acetate for 1 min and examined under a Hitachi H-7600 transmission electron microscope. To prepare thin sections of HCV-LPs, we prefixed precipitated HCV-LPs in 2% glutaraldehyde–0.1 M cacodylate buffer at 4 °C overnight, followed by three rounds of washing with 0.1 M cacodylate buffer. The samples were then postfixed in 2% osmium tetroxide at 4 °C for 2 h, dehydrated in a graded series of ethanol solutions followed by propylene oxide, and embedded in a mixture of EPON 812, dodecenyl succinic anhydride (DDSA), methyl nadic anhydrate (MNA), and 2,4,6-tri (dimethylaminomethyl) phenol (DMP-30) at 60 °C for 2 days. Thin sections (80 nm) were stained with uranyl acetate and lead citrate. For electron microscopy of RCYM1 cells cultured in TGP, the cells were prefixed in 2% glutaraldehyde–0.1 M cacodylate buffer at 4 °C for 1 h and washed three times with 0.1 M cacodylate buffer, followed by postfixation in 2% osmium tetroxide for 3 h. After dehydration in a graded series of ethanol solutions and propylene oxide, the cells were embedded in a mixture of Epoxy 812, DDSA, MNA, and DMP-30 at 60 °C for 2 days. Thin sections (60–80 nm) were stained with 2% uranyl acetate.

Immunoelectron microscopy

HCV-LP samples were adsorbed on formvar-carbon grids and then floated for 30 min on a drop of BlockAce. Diluted anti-E2 mouse antibody was then applied for 1 h. After three rounds of washing, diluted anti-mouse IgG conjugated with 5-nm gold particles was applied for 1 h, and the grids were then stained with 1% uranyl acetate. In order to perform immunoelectron microscopy of TGP cultures using silver-intensified immunogold labeling, we fixed the cells in 4% paraformaldehyde–0.1% glutaraldehyde with 0.15 M HEPES buffer at 4 °C, followed by incubation with either anti-core rabbit antibody or anti-E1 mouse antibody overnight. After several washings, anti-rabbit or anti-mouse secondary antibody coupled with 1.4-nm-diameter gold particles (Nanoprobes) was applied overnight. The samples were then washed and fixed in 2% glutaraldehyde in 0.1 M sodium cacodylate buffer (pH 7.4) for 3 h, followed by enlargement of the gold particles with an HQ-Silver Enhancement Kit (Nanoprobes). For double staining with anti-E1 and anti-core antibodies, the cells were fixed in 7% paraformaldehyde–0.25 M sucrose in 0.03% picric acid–0.05 M cacodylate buffer at pH 7.4. Ten-nanometer gold particle-coupled anti-rabbit and 5-nm gold particle-coupled anti-mouse antibodies were used as secondary antibodies.

Assays for the infectivity of HCV-LPs and neutralization of the infection

Cell supernatant from 3D-cultured RCYM1 cells was centrifuged at 8000 × *g* for 50 min to remove all cellular debris, after which the supernatant was centrifuged at 25,000 rpm at 4 °C for 4 h with an SW28 rotor. The precipitant was suspended in 0.2–0.5 ml of ASF104 medium and the aliquot containing approximately 1×10^5 HCV RNA copies was used as each inoculum. Huh-7.5.1

cells (provided by Dr. F. V. Chisari, The Scripps Research Institute) (Zhong et al., 2005), which were seeded at a density of 10^4 cells/well in a 48-well plate 24 h before infection. The inocula were incubated for 3 h, followed by 3 rounds of washing with PBS and the addition of complete medium. For the kinetics assay, cells were harvested 0, 1, 2, 3, and 7 days after infection and the amount of intracellular HCV RNA was quantified as described above. Infection with HCV-LP was determined after 4 days by immunofluorescence staining for HCV NS5A. In the neutralization assay, the HCV-LP samples were incubated with the anti-E2 antibody AP33 (Owsianka et al., 2005) at 10 μg/ml (kindly provided by Dr. A. H. Patel, University of Glasgow, UK), with the human sera with high titers of NOB antibodies NOB3 and NOB4 (Ishii et al., 1998), or with anti-FLAG antibody (Sigma) at 10 μg/ml for 1 h at 37 °C prior to infection. Anti-human CD81 antibody (BD Pharmigen) at 10 μg/ml was preincubated with Huh-7.5.1 cells for 1 h at 37 °C, followed by being washed with PBS three times. HCV-LP derived from TGP-cultured RCYM1 cells or JFH1 virus was incubated with these cells, as mentioned above. JFH1 virus was prepared from pJFH1 (Wakita et al., 2005), which contains the full-length cDNA of JFH1 isolate and was kindly provided by T. Wakita (Tokyo Metropolitan Institute for Neuroscience, Japan), as described (Wakita et al., 2005). The cells were harvested 4 days after infection and neutralizing activity was assessed by quantifying the amount of intracellular HCV RNA as described above.

Assay for anti-HCV-LP production

At the initiation of the 3D culture of RCYM1 cells (5×10^5 in 1 ml TGP), 100 IU/ml IFN-α (Sumiferon 300; Sumitomo Pharmaceuticals, Japan), or 100 μM RBV (MP Biomedicals, Germany) were added and the cells were cultured for 5 days. Culture media were harvested and fractionated by sucrose density centrifugation as described above. Total RNAs were extracted from aliquots of 1.18 g/ml (HCV-LP positive) and 1.04 g/ml (HCV-LP-negative) fractions, followed by quantification of viral RNA.

Acknowledgments

The authors would like to thank Francis V. Chisari of The Scripps Research Institute, Arvind H. Patel of the University of Glasgow, and Takaji Wakita of Tokyo Metropolitan Institute for Neuroscience for providing Huh-7.5.1 cells, anti-E2 antibody, and pJFH1, respectively. We also thank Mami Matsuda, Tetsu Shimoji, and Makiko Yahata for technical assistance, and Tomoko Mizoguchi for her secretarial work. This work was supported in part by a grant for Research on Health Sciences focusing on Drug Innovation from the Japan Health Sciences Foundation; by grants-in-aid from the Ministry of Health, Labor and Welfare; by a Sasagawa Scientific Research Grant from the Japan Science Society; and by the program for Promotion of Fundamental Studies in Health Sciences of the National Institute of Biomedical Innovation (NBIO), Japan; and by the New Energy and Industrial Technology Development Organization (NEDO) of Japan.

References

Aizaki, H., Nagamori, S., Matsuda, M., Kawakami, H., Hashimoto, O., Ishiko, H., Kawada, M., Matsuura, T., Hasumura, S., Matsuura, Y., Suzuki, T., Miyamura, T., 2003. Production and release of infectious hepatitis C virus from human liver cell cultures in the three-dimensional radial-flow bioreactor. Virology 314, 16–25.

Aizaki, H., Lee, K.J., Sung, V.M., Ishiko, H., Lai, M.M., 2004. Characterization of the hepatitis C virus RNA replication complex associated with lipid rafts. Virology 324, 450–461.

Andre, P., Komurian-Pradel, F., Deforges, S., Perret, M., Berland, J.L., Sodoyer, M., Pol, S., Brechot, C., Paranhos-Baccala, G., Lotteau, V., 2002. Characterization of low- and very-low-density hepatitis C virus RNA-containing particles. J. Virol. 76, 6919–6928.

Bartosch, B., Cosset, F.L., 2006. Cell entry of hepatitis C virus. Virology (Electronic publication ahead of print).

Baumert, T.F., Ito, S., Wong, D.T., Liang, T.J., 1998. Hepatitis C virus structural proteins assemble into viruslike particles in insect cells. J. Virol. 72, 3827–3836.

Blanchard, E., Brand, D., Trassard, S., Goudeau, A., Roingeard, P., 2002. Hepatitis C virus-like particle morphogenesis. J. Virol. 76, 4073–4079.

Blanchard, E., Hourioux, C., Brand, D., Ait-Goughoulte, M., Moreau, A., Trassard, S., Sizaret, P.Y., Dubois, F., Roingeard, P., 2003. Hepatitis C virus-like particle budding: role of the core protein and importance of its Asp111. J. Virol. 77, 10131–10138.

Blight, K.J., Kolykhalov, A.A., Rice, C.M., 2000. Efficient initiation of HCV RNA replication in cell culture. Science 290, 1972–1974.

Blight, K.J., McKeating, J.A., Rice, C.M., 2002. Highly permissive cell lines for subgenomic and genomic hepatitis C virus RNA replication. J. Virol. 76, 13001–13014.

Bruno, S., Silini, E., Crosignani, A., Borzio, F., Leandro, G., Bono, F., Asti, M., Rossi, S., Larghi, A., Cerino, A., Podda, M., Mondelli, M.U., 1997. Hepatitis C virus genotypes and risk of hepatocellular carcinoma in cirrhosis: a prospective study. Hepatology 25, 754–758.

Choo, Q.L., Kuo, G., Weiner, A.J., Overby, L.R., Bradley, D.W., Houghton, M., 1989. Isolation of a cDNA clone derived from a blood-borne non-A, non-B viral hepatitis genome. Science 244, 359–362.

Choo, Q.L., Richman, K.H., Han, J.H., Berger, K., Lee, C., Dong, C., Gallegos, C., Coit, D., Medina-Selby, R., Barr, P.J., et al., 1991. Genetic organization and diversity of the hepatitis C virus. Proc. Natl. Acad. Sci. U.S.A. 88, 2451–2455.

Compans, R.W., 1995. Virus entry and release in polarized epithelial cells. Curr. Top. Microbiol. Immunol. 202, 209–219.

Date, T., Kato, T., Miyamoto, M., Zhao, Z., Yasui, K., Mizokami, M., Wakita, T., 2004. Genotype 2a hepatitis C virus subgenomic replicon can replicate in HepG2 and IMY-N9 cells. J. Biol. Chem. 279, 22371–22376.

Davis, G.L., Wong, J.B., McHutchison, J.G., Manns, M.P., Harvey, J., Albrecht, J., 2003. Early virologic response to treatment with peginterferon alfa-2b plus ribavirin in patients with chronic hepatitis C. Hepatology 38, 645–652.

Frese, M., Pietschmann, T., Moradpour, D., Haller, O., Bartenschlager, R., 2001. Interferon-alpha inhibits hepatitis C virus subgenomic RNA replication by an MxA-independent pathway. J. Gen. Virol. 82, 723–733.

Garoff, H., Hewson, R., Opstelten, D.J., 1998. Virus maturation by budding. Microbiol. Mol. Biol. Rev. 62, 1171–1190.

Grakoui, A., McCourt, D.W., Wychowski, C., Feinstone, S.M., Rice, C.M., 1993. Characterization of the hepatitis C virus-encoded serine proteinase: determination of proteinase-dependent polyprotein cleavage sites. J. Virol. 67, 2832–2843.

Guo, J.T., Bichko, V.V., Seeger, C., 2001. Effect of alpha interferon on the hepatitis C virus replicon. J. Virol. 75, 8516–8523.

Heller, T., Saito, S., Auerbach, J., Williams, T., Moreen, T.R., Jazwinski, A., Cruz, B., Jeurkar, N., Sapp, R., Luo, G., Liang, T.J., 2005. An in vitro model of hepatitis C virion production. Proc. Natl. Acad. Sci. U.S.A. 102, 2579–2583.

Hijikata, M., Kato, N., Ootsuyama, Y., Nakagawa, M., Shimotohno, K., 1991. Gene mapping of the putative structural region of the hepatitis C virus genome by in vitro processing analysis. Proc. Natl. Acad. Sci. U.S.A. 88, 5547–5551.

Hishikawa, K., Miura, S., Marumo, T., Yoshioka, H., Mori, Y., Takato, T., Fujita, T., 2004. Gene expression profile of human mesenchymal stem cells during osteogenesis in three-dimensional thermoreversible gelation polymer. Biochem. Biophys. Res. Commun. 317, 1103–1107.

Ikeda, M., Yi, M., Li, K., Lemon, S.M., 2002. Selectable subgenomic and genome-length dicistronic RNAs derived from an infectious molecular clone of the HCV-N strain of hepatitis C virus replicate efficiently in cultured Huh7 cells. J. Virol. 76, 2997–3006.

Ishii, K., Rosa, D., Watanabe, Y., Katayama, T., Harada, H., Wyatt, C., Kiyosawa, K., Aizaki, H., Matsuura, Y., Houghton, M., Abrignani, S., Miyamura, T., 1998. High titers of antibodies inhibiting the binding of envelope to human cells correlate with natural resolution of chronic hepatitis C. Hepatology 28, 1117–1120.

Iwahori, T., Matsuura, T., Maehashi, H., Sugo, K., Saito, M., Hosokawa, M., Chiba, K., Masaki, T., Aizaki, H., Ohkawa, K., Suzuki, T., 2003. CYP3A4 inducible model for in vitro analysis of human drug metabolism using a bioartificial liver. Hepatology 37, 665–673.

Kanto, T., Hayashi, N., Takehara, T., Hagiwara, H., Mita, E., Naito, M., Kasahara, A., Fusamoto, H., Kamada, T., 1994. Buoyant density of hepatitis C virus recovered from infected hosts: two different features in sucrose equilibrium density-gradient centrifugation related to degree of liver inflammation. Hepatology 19, 296–302.

Kato, T., Furusaka, A., Miyamoto, M., Date, T., Yasui, K., Hiramoto, J., Nagayama, K., Tanaka, T., Wakita, T., 2001. Sequence analysis of hepatitis C virus isolated from a fulminant hepatitis patient. J. Med. Virol. 64, 334–339.

Kato, T., Date, T., Miyamoto, M., Furusaka, A., Tokushige, K., Mizokami, M., Wakita, T., 2003. Efficient replication of the genotype 2a hepatitis C virus subgenomic replicon. Gastroenterology 125, 1808–1817.

Kawada, M., Nagamori, S., Aizaki, H., Fukaya, K., Niiya, M., Matsuura, T., Sujino, H., Hasumura, S., Yashida, H., Mizutani, S., Ikenaga, H., 1998. Massive culture of human liver cancer cells in a newly developed radial flow bioreactor system: ultrafine structure of functionally enhanced hepatocarcinoma cell lines. In Vitro Cell. Dev. Biol. Anim. 34, 109–115.

Kleinman, H.K., McGarvey, M.L., Hassell, J.R., Star, V.L., Cannon, F.B., Laurie, G.W., Martin, G.R., 1986. Basement membrane complexes with biological activity. Biochemistry 25, 312–318.

Lawler, E.M., Miller, F.R., Heppner, G.H., 1983. Significance of three-dimensional growth patterns of mammary tissues in collagen gels. In Vitro 19, 600–610.

Lindenbach, B.D., Evans, M.J., Syder, A.J., Wolk, B., Tellinghuisen, T.L., Liu, C.C., Maruyama, T., Hynes, R.O., Burton, D.R., McKeating, J.A., Rice, C.M., 2005. Complete replication of hepatitis C virus in cell culture. Science 309, 623–626.

Lohmann, V., Korner, F., Koch, J., Herian, U., Theilmann, L., Bartenschlager, R., 1999. Replication of subgenomic hepatitis C virus RNAs in a hepatoma cell line. Science 285, 110–113.

Manns, M.P., McHutchison, J.G., Gordon, S.C., Rustgi, V.K., Shiffman, M., Reindollar, R., Goodman, Z.D., Koury, K., Ling, M., Albrecht, J.K., 2001. Peginterferon alfa-2b plus ribavirin compared with interferon alfa-2b plus ribavirin for initial treatment of chronic hepatitis C: a randomised trial. Lancet 358, 958–965.

Matsuura, T., Kawada, M., Hasumura, S., Nagamori, S., Obata, T., Yamaguchi, M., Hataba, Y., Tanaka, H., Shimizu, H., Unemura, Y., Nonaka, K., Iwaki, T., Kojima, S., Aizaki, H., Mizutani, S., Ikenaga, H., 1998. High density culture of immortalized liver endothelial cells in the radial-flow bioreactor in the development of an artificial liver. Int. J. Artif. Organs 21, 229–234.

Nagaya, M., Kubota, S., Suzuki, N., Tadokoro, M., Akashi, K., 2004. Evaluation of thermoreversible gelation polymer for regeneration of focal liver injury. Eur. Surg. Res. 36, 95–103.

Nakajima, N., Hijikata, M., Yoshikura, H., Shimizu, Y.K., 1996. Characterization of long-term cultures of hepatitis C virus. J. Virol. 70, 3325–3329.

Netski, D.M., Mosbruger, T., Depla, E., Maertens, G., Ray, S.C., Hamilton, R.G., Roundtree, S., Thomas, D.L., McKeating, J., Cox, A., 2005. Humoral immune response in acute hepatitis C virus infection. Clin. Infect. Dis. 41, 667–675.

Owsianka, A., Tarr, A.W., Juttla, V.S., Lavillette, D., Bartosch, B., Cosset, F.L., Ball, J.K., Patel, A.H., 2005. Monoclonal antibody AP33 defines a broadly neutralizing epitope on the hepatitis C virus E2 envelope glycoprotein. J. Virol. 79, 11095–11104.

Pietschmann, T., Lohmann, V., Rutter, G., Kurpanek, K., Bartenschlager, R., 2001. Characterization of cell lines carrying self-replicating hepatitis C virus RNAs. J. Virol. 75, 1252–1264.

Pietschmann, T., Lohmann, V., Kaul, A., Krieger, N., Rinck, G., Rutter, G., Strand, D., Bartenschlager, R., 2002. Persistent and transient replication of full-length hepatitis C virus genomes in cell culture. J. Virol. 76, 4008–4021.

Pileri, P., Uematsu, Y., Campagnoli, S., Galli, G., Falugi, F., Petracca, R., Weiner, A.J., Houghton, M., Rosa, D., Grandi, G., Abrignani, S., 1998. Binding of hepatitis C virus to CD81. Science 282, 938–941.

Rosa, D., Campagnoli, S., Moretto, C., Guenzi, E., Cousens, L., Chin, M., Dong, C., Weiner, A.J., Lau, J.Y., Choo, Q.L., Chien, D., Pileri, P., Houghton, M., Abrignani, S., 1996. A quantitative test to estimate neutralizing antibodies to the hepatitis C virus: cytofluorimetric assessment of envelope glycoprotein 2 binding to target cells. Proc. Natl. Acad. Sci. U.S.A. 93, 1759–1763.

Sasaki, M., Yamauchi, K., Nakanishi, T., Kamogawa, Y., Hayashi, N., 2003. In vitro binding of hepatitis C virus to CD81-positive and -negative human cell lines. J. Gastroenterol. Hepatol. 18, 74–79.

Schmitt, A.P., Lamb, R.A., 2004. Escaping from the cell: assembly and budding of negative-strand RNA viruses. Curr. Top. Microbiol. Immunol. 283, 145–196.

Shimizu, Y.K., Feinstone, S.M., Kohara, M., Purcell, R.H., Yoshikura, H., 1996. Hepatitis C virus: detection of intracellular virus particles by electron microscopy. Hepatology 23, 205–209.

Silini, E., Bottelli, R., Asti, M., Bruno, S., Candusso, M.E., Brambilla, S., Bono, F., Iamoni, G., Tinelli, C., Mondelli, M.U., Ideo, G., 1996. Hepatitis C virus genotypes and risk of hepatocellular carcinoma in cirrhosis: a case–control study. Gastroenterology 111, 199–205.

Suzuki, T., Omata, K., Satoh, T., Miyasaka, T., Arai, C., Maeda, M., Matsuno, T., Miyamura, T., 2005. Quantitative detection of hepatitis C virus (HCV) RNA in saliva and gingival crevicular fluid of HCV-infected patients. J. Clin. Microbiol. 43, 4413–4417.

Takimoto, T., Portner, A., 2004. Molecular mechanism of paramyxovirus budding. Virus Res. 106, 133–145.

Trestard, A., Bacq, Y., Buzelay, L., Dubois, F., Barin, F., Goudeau, A., Roingeard, P., 1998. Ultrastructural and physicochemical characterization of the hepatitis C virus recovered from the serum of an agammaglobulinemic patient. Arch. Virol. 143, 2241–2245.

Wakita, T., Pietschmann, T., Kato, T., Date, T., Miyamoto, M., Zhao, Z., Murthy, K., Habermann, A., Krausslich, H.G., Mizokami, M., Bartenschlager, R., Liang, T.J., 2005. Production of infectious hepatitis C virus in tissue culture from a cloned viral genome. Nat. Med. 11, 791–796.

Yi, M.K., Villanueva, R.A., Thomas, D., Wakita, T., Lemon, S.M., 2006. Production of infectious genotype 1a hepatitis C virus (Hutchinson strain) in cultured human hepatoma cells. Proc. Natl. Acad. Sci. U.S.A. 103, 2310–2315.

Yoshioka, H., Mikami, M., Mori, Y., Tsuchida, E., 1994. A synthetic hydrogel with thermoreversible gelation. J. Macromol. Sci. A31, 113–120.

Zhong, J., Gastaminza, P., Cheng, G., Kapadia, S., Kato, T., Burton, D.R., Wieland, S.F., Uprichard, S.L., Wakita, T., Chisari, F.V., 2005. Robust hepatitis C virus infection in vitro. Proc. Natl. Acad. Sci. U.S.A. 102, 9294–9299.

J. Biochem. 139, 921–930 (2006)
doi:10.1093/jb/mvj104

Proteomic Profiling of Lipid Droplet Proteins in Hepatoma Cell Lines Expressing Hepatitis C Virus Core Protein

Shigeko Sato[1], Masayoshi Fukasawa[1,*], Yoshio Yamakawa[1], Tohru Natsume[2], Tetsuro Suzuki[3], Ikuo Shoji[3], Hideki Aizaki[3], Tatsuo Miyamura[3] and Masahiro Nishijima[1,†]

[1]Department of Biochemistry and Cell Biology and [3]Department of Virology II, National Institute of Infectious Diseases, Tokyo 162-8640; and [2]National Institute of Advanced Industrial Science and Technology (AIST), Biological Information Research Center, Tokyo 135-0064

Received February 7, 2006; accepted April 4, 2006

Hepatitis C virus (HCV) core protein has been suggested to play crucial roles in the pathogeneses of liver steatosis and hepatocellular carcinomas due to HCV infection. Intracellular HCV core protein is localized mainly in lipid droplets, in which the core protein should exert its significant biological/pathological functions. In this study, we performed comparative proteomic analysis of lipid droplet proteins in core-expressing and non-expressing hepatoma cell lines. We identified 38 proteins in the lipid droplet fraction of core-expressing (Hep39) cells and 30 proteins in that of non-expressing (Hepswx) cells by 1-D-SDS-PAGE/MALDI-TOF mass spectrometry (MS) or direct nanoflow liquid chromatography–MS/MS. Interestingly, the lipid droplet fraction of Hep39 cells had an apparently lower content of adipose differentiation–related protein and a much higher content of TIP47 than that of Hepswx cells, suggesting the participation of the core protein in lipid droplet biogenesis in HCV-infected cells. Another distinct feature is that proteins involved in RNA metabolism, particularly DEAD box protein 1 and DEAD box protein 3, were detected in the lipid droplet fraction of Hep39 cells. These results suggest that lipid droplets containing HCV core protein may participate in the RNA metabolism of the host and/or HCV, affecting the pathopoiesis and/or virus replication/production in HCV-infected cells.

Key words: ADRP, DEAD box protein, hepatitis C virus, lipid droplet, TIP47.

Abbreviations: HCV, hepatitis C virus; HCC, hepatocellular carcinoma; MS, mass spectrometry; DNLC, direct nanoflow liquid chromatography; HRP, horseradish peroxidase; ADRP, adipose differentiation–related protein; DDX1, DEAD box protein 1; DDX3, DEAD box protein 3.

Hepatitis C virus (HCV) is a major causative agent of chronic hepatitis (*1*, *2*). Persistent HCV infection, which occurs in more than 70% of infected patients, is strongly associated with the development of liver steatosis, which involves the accumulation of intracellular lipid droplets, cirrhosis, and hepatocellular carcinomas (HCC) (*3*, *4*). Since more than 170 million people in the world are currently infected with HCV (*1*), and there is no cure that is completely effective, understanding the mechanism by which HCV induces serious liver diseases is one of the most important global public health issues. HCV, a member of the *Flaviviridae* family, possesses a single-stranded, positive-sense RNA genome of ~9.6 kb (*5*). The HCV genome has a single open reading frame that codes for a large precursor polyprotein of ~3,000 amino acids that is processed into at least 10 individual proteins by host and viral proteases (*6*).

HCV core protein, the product of the N-terminal portion of the polyprotein, generated upon cleavage at the endoplasmic reticulum by signal peptidase and signal peptide peptidase (*7*, *8*), forms the nucleocapsid of an HCV virion (*9*). Interestingly, in addition to its function as a structural protein, the core protein exhibits activities leading host cells to lipogenic and malignant transformation *in vitro* (*10–12*). Moreover, transgenic mice expressing HCV core protein developed liver steatosis and HCC (*13*, *14*), suggesting an important role of the core protein in these diseases. Many studies have shown that HCV core protein substantially affects various cellular regulatory processes, such as gene transcription (*15–17*) and signal transduction pathways (*12*, *18–23*), and interacts with a variety of host proteins (*12*, *18*, *19*, *22*, *24–34*), but it is not clear what activities/molecules are practically relevant to the pathogeneses of HCV (core)-derived liver steatosis and HCC. Extensive screenings for genes/proteins exhibiting differences in cellular expression by cDNA microarray (*35–40*) or proteome analysis (*41*, *42*) have also been tried for HCV-related HCC. Although various genes/proteins were identified, further studies are required to identify the molecules eventually involved in the pathogenesis of HCV-related HCC.

In host cells, HCV core protein is distributed mainly in lipid droplets and the endoplasmic reticulum (*7*, *10*, *43–46*), in which the core protein is predicted to exert its significant biological/pathological functions. In this study, we thus focused on HCV core protein and lipid droplets, and

*To whom correspondence should be addressed. Tel: +81-3-5285-1111, Fax: +81-3-5285-1157, E-mail: fuka@nih.go.jp
†Present address: Department of Clinical Pharmacy, Faculty of Pharmaceutical Sciences, Doshisha Women's College of Liberal Arts, Kyoto 610-0395.

performed comparative targeted proteomic analysis of the lipid droplet proteins in HCV core–expressing and non-expressing hepatoma cell lines using two strategies: conventional 1-D-SDS-PAGE/MALDI-TOF mass spectrometry (MS) and automated high-throughput direct nanoflow liquid chromatography (DNLC)–MS/MS. We found prominent differences in the protein compositions of lipid droplets between HCV core–expressing and non-expressing hepatoma cell lines.

MATERIALS AND METHODS

Cell Lines—The human hepatoma HepG2 cell line constitutively expressing HCV core protein (Hep39) was established as described previously (*47*). Another HepG2 cell line transfected with expression vector pcEF321swxneo without the HCV core protein insert (Hepswx) was used as a mock control (*47*). Both cell lines were plated on collagen-coated dishes (Asahi Techno Glass, Tokyo, Japan) and maintained in the normal culture medium [DMEM supplemented with 10% fetal bovine serum, 100 units/ml Penicillin G, 100 μg/ml streptomycin sulfate, and 1 mg/ml G418 (Sigma, St. Louis, MO, USA)] under a 5% CO_2 atmosphere at 37°C.

Lipid Droplet Preparation—Hepswx and Hep39 cells were seeded at 4×10^6 cells/dish (150 mm, inner diameter) in 25 ml of normal culture medium and cultured for one day. For efficient formation of lipid droplets by cells, cholesterol (final 20 μg/ml) and oleic acid (final 400 μM)/fatty acid–free BSA (final 60 μM) complex, prepared as stock solutions of 5 mg/ml cholesterol in ethanol and 10 mM oleic acid/1.5 mM BSA in PBS, respectively, were added to the medium. Each cell line was further incubated for 48–72 h at 37°C. For proteomic analysis of lipid droplet proteins, confluent monolayers of Hepswx and Hep39 cells in fifteen cell culture dishes (150 mm, inner diameter) were harvested by scraping and pelleted by centrifugation ($200 \times g$ for 5 min at 4°C). After being washed with PBS three times, each cell pellet was resuspended in 10 mM Tris-HCl buffer, pH 7.5, containing 0.25 M sucrose and Complete™, EDTA-free (Roche, Mannheim, Germany) to achieve a final volume equal to five times the volume of the cell pellet (*i.e.* a 20% cell suspension). The cell suspension was homogenized with a ball-bearing homogenizer (*48*), and then centrifuged at $800 \times g$ for 5 min at 4°C. One milliliter of each post-nuclear supernatant fraction was layered under 2 ml of 10 mM Tris-HCl buffer, pH 7.5, containing 0.15 M NaCl (TN-buffer). After centrifugation at $100{,}000 \times g$ for 60 min at 4°C, the lipid droplet fraction, *i.e.* the distinct white band on the top of the preparation, was collected with a pipetman. The floating lipid droplet fraction was diluted with 3.5 ml of TN-buffer and then re-purified by centrifugation ($100{,}000 \times g$ for 30 min at 4°C). This washing step was repeated three times. Lipid droplets in the floating fractions in both cells were enriched up to more than 500-fold compared with those in the total cell lysates as estimated by their protein contents. The amounts of lipid droplets isolated from Hepswx and Hep39 cells were nearly the same. The purified lipid droplet fractions (~0.1 mg of protein per ml) were stored at −80°C until use. The purity of the lipid droplet fractions was verified by microscopic and immunoblot (Fig. 1) analyses. Adipose differentiation–related protein (ADRP), a known lipid droplet protein, was significantly enriched in the lipid droplet fractions of Hepswx and Hep39 cells (Fig. 1). Other organelle marker proteins, such as nucleoporin p62 for the nucleus, prohibitin for the mitochondria, fatty acid synthase for the cytoplasm, GM130 for the Golgi apparatus, EEA1 for the early endosome, or annexin II for the plasma membrane, were not detected in the lipid droplet fractions of either cells (Fig. 1). Small amounts of calnexin, a marker of the endoplasmic reticulum, which is a major organelle, were detected in the lipid droplet fractions of both cells to a similar extent. Although we did not detect calnexin in the lipid droplet fractions by proteomic analysis (see Tables 1 and 2), the lipid droplet fractions of both cells could be contaminated with a small amount of endoplasmic reticulum.

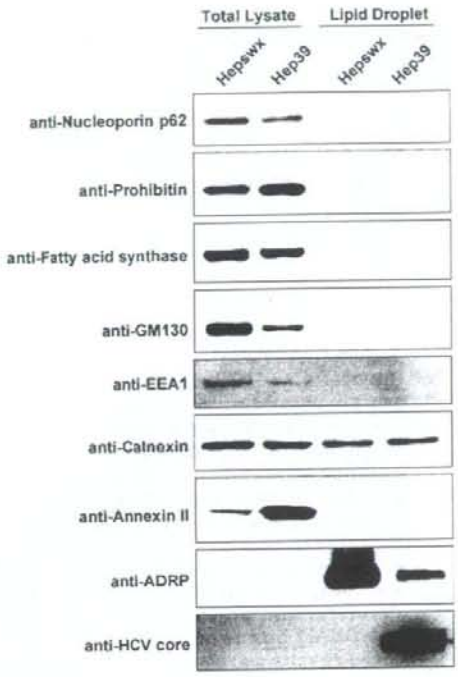

Fig. 1. **Immunoblot analysis of lipid droplet fractions in Hepswx and Hep39 cells using antibodies against various organelle markers.** Total cell lysates and lipid droplet fractions (1.5 μg of protein per lane in the case of anti-ADRP; 5 μg of protein per lane in others) from Hepswx and Hep39 cells were analyzed by immunoblotting with the indicated antibodies.

1-D-SDS-PAGE/MALDI-TOF MS Analysis—The lipid droplet fraction (30 μg protein) of each cell line was fractionated in a 10% SDS–polyacrylamide gel, and the gel was stained with Coomassie Brilliant Blue. The protein bands were excised from the gel and subjected to in-gel trypsin digestion. The tryptic peptide mixtures were analyzed by MALDI-TOF MS as described previously (*49*). Prior to MALDI-TOF MS analysis, the peptide mixtures were desalted using C18 Zip Tips (Millipore, Billerica, MA, USA) according to the manufacturer's instructions. The peptide data were collected in the reflection mode and with positive polarity, using a saturated solution of

Table 1. **Lipid droplet proteins identified in Hepswx and Hep39 cells by means of 1-D-SDS-PAGE/MALDI-TOF MS.**

Protein	Molecular mass (kDa) (calc.)	Accession No.	SDS band No.[a]	
			Hepswx	Hep39
PAT family proteins				
Adipose differentiation–related protein (ADRP)	48.1	34577059	5	21
Cargo selection protein/TIP47	47.0	20127486		22
Lipid metabolism				
Acyl CoA synthetase long chain family member 3	80.4	42794752	4	18
Cytochrome b_5 reductase	34.3	4503327	9	26
Lanosterol synthase	83.3	4808278	4	18
NAD(P)-dependent steroid dehydrogenase-like; H105e3	41.9	8393516	8	25
Retinal short-chain dehydrogenase/reductase retSDR2	33.0	7705905	10	27
Cytosolic phospholipase A_2	85.2	1352707		14
Rab GTPases				
Rab1A	22.7	4758988	13	30
Rab1B	22.2	23396834	13	30
Rab5C	23.5	38258923	11	28
Rab7	23.5	34147513	12	29
RNA metabolism/binding				
DEAD box protein 1 (DDX1)	82.9	6919862		16
DEAD box protein 3 (DDX3)	73.2	3023628		18
HC56/gemin 4	118.8	10945430		15
Other/unknown proteins				
BiP protein	70.9	14916999	3	17
CGI-49 protein	46.9	7705767	6	23
Heat shock protein gp96 precursor	90.2	15010550	2	14
Ancient ubiquitous protein 1	41.4	31712024	7	
Major vault protein	99.3	15990478	1	
Apoptosis-inducing factor–homologous mitochondrion-associated inducer of death	40.5	13543964		24
KIAA0887 protein	52.4	4240263		21
Protein disulfide-isomerase [EC 5.3.4.1] ER60 precursor	56.7	1085373		20
Transport-secretion protein 2.1	57.7	9663151		19
HCV core protein	20.6	974345		31

[a]Band numbers correspond to those in Fig. 2.

α-cyano-4-hydroxycinnamic acid (Sigma) in 50% acetonitrile and 0.1% trifluoroacetic acid as the matrix. Spectra were obtained using a Voyager DE-STR MALDI-TOF mass spectrometer (PE Biosystems, Foster City, CA, USA). Internal calibration was performed with adrenocorticotropic hormone, fragment 18–39 (Sigma), and bradykinin fragment (Sigma). The data base–fitting program MS-Fit available at the WWW site of the University of California, San Francisco (prospector.ucsf.edu/ucsfhtml3.4/msfit.htm) was used to interpret the MS spectra of protein digests (*50*).

DNLC-MS/MS Analysis—The lipid droplet fraction (10 μg protein) of each cell line was first delipidated by chloroform–methanol extraction as originally described (*51*). Two volumes of chloroform and 1 volume of methanol were mixed with 0.8 volume of the lipid droplet fraction. Then, 1 volume of chloroform and 1 volume of water were added to the mixture, and the mixture was vortexed for 30 s, and centrifuged at 10,000 × *g* for 5 min at room temperature. The resulting organic (lower) phase was removed. The aqueous (upper) phase and interface, containing all the lipid droplet proteins, was lyophilized. The delipidated lipid droplet proteins were digested with endoproteinase Lys-C, and the resulting peptides were analyzed by DNLC-MS/MS as described (*52*, *53*).

Cell Fractionation—All manipulations were performed at 4°C or on ice. After being washed with PBS, confluent monolayers of Hepswx and Hep39 cells were harvested by scraping and pelleted by centrifugation (200 × *g*, 5 min). The precipitated cells were homogenized with a ball-bearing homogenizer in 10 mM Tris-HCl buffer, pH 7.5, containing 0.25 M sucrose, and Complete™, EDTA-free. After centrifugation of the lysate at 800 × *g* for 5 min, the cytosolic fraction (100,000 × *g* supernatant) and membrane fraction (100,000 × *g* precipitate) were separated from the post-nuclear supernatant fraction by centrifugation at 100,000 × *g* for 60 min. The membrane fraction was resuspended in TN-buffer and then re-purified twice by centrifugation. The protein concentrations of these preparations were determined with BCA protein assay reagents (Pierce Biotechnology, Rockford, IL, USA) using BSA as a standard.

Immunoblot Analysis—Equivalent amounts of proteins from Hepswx and Hep39 cells were separated in a 10 or 12.5% SDS–polyacrylamide gel and then electrophoretically transferred to a polyvinylidene difluoride membrane. The membranes were blocked overnight at 4°C or 30 min at room temperature in TBS containing 0.1% Tween 20 and 5% skim milk. The blots were probed with a mouse

Table 2. **Lipid droplet proteins identified in Hepswx and Hep39 cells by means of DNLC-MS/MS.**

Protein	Accession No.	Molecular mass (kDa) (calc.)	Matched peptide sequence	
			Hepswx[a]	Hep39[a]
PAT family proteins				
Adipose differentiation–related protein (ADRP)	34577059	48.1	+ TITSVAMTSALPIIQK DAVTTTVTGAK EVSDSLLTSSK	+ TITSVAMTSALPIIQK DAVTTTVTGAK EVSDSLLTSSK
Cargo selection protein / TIP47	20127486	47.0	+ VSGAQEMVSSAK	+ VSGAQEMVSSAK
Lipid metabolism				
Acyl-CoA synthetase long-chain family member 3	42794752	80.4	+ VLSEAAISASLEK	+ ELTELARK
Cytochrome b_5 reductase	4503327	34.2	+ DILLRPELEELRNK	+ SNPIIRTVK
Gastric-associated differentially-expressed protein YA61P	6970062	14.9	+ AIGLVVPSLTGK	+ AIGLVVPSLTGK
Retinal short-chain dehydrogenase/reductase retSDR2	7705905	33.0	+ HGLEETAAK	+ FDAVIGYK
Sterol carrier protein 2–related form, 58.85K	86717	58.8	+ LQNLQLQPGNAK	+ LQNLQLQPGNAK
Acyl-CoA synthetase long-chain family member 4	4758332	74.4	+ SDQSYVISFVVPNQK	
Fatty acid binding protein 5	4557581	15.2	+ ELGVGIALRK	
Hydroxysteroid (17-beta) dehydrogenase 4	4504505	79.7		+ NHPMTPEAVK
Rab GTPases				
Rab1A	4758988	22.6	+[b] QWLQEIDRYASENVNK RMGPGATAGGAEK	+ RMGPGATAGGAEK
Rab1B	23396834	22.1	+[b] QWLQEIDRYASENVNK	+ RMGPGAASGGERPNLK
Rab7	34147513	23.5	+ NNIPYFETSAK	+ ATIGADFLTK
Rab18	20809384	22.9	+ HSMLFIEASAK	+ ILIIGESGVGK
Rab10	12654157	22.5	+ LLLIGDSGVGK	
Rab11	4758986	24.5	+ VVLIGDSGVGK	
Rab8	539607	23.6		+ IRTIELDGK
RNA metabolism/binding				
DEAD box protein 1 (DDX1)	6919862	82.4		+ FGFGFGGTGK
DEAD box protein 3 (DDX3)	3023628	73.2		+ GVRHTMMFSATFPK
IGF-II mRNA-binding protein 3	30795212	63.7		+ EGATIRNITK
Ribosomal protein L29	14286258	17.8		+ AQAAAPASVPAQAPK
Other/unknown proteins				
Apoptosis-inducing factor homologous mitochondrion-associated inducer of death	13543964	40.5	+ EVTLIHSQVALADK	+ EVTLIHSQVALADK
BiP protein	14916999	72.3	+ SQIFSTASDNQPTVTIK	+ VYEGERPLTK
Hypothetical protein DKFZp586A0522.1	7512845	28.2	+ LQHIQAPLSWELVRPH-IYGYAVK	+ RELFSNLQEFAGPSGK
Prolyl 4-hydroxylase, beta subunit	20070125	57.1	+ VHSFPTLK	+ AEGSEIRLAK
Ancient ubiquitous protein 1	31712024	41.4	+ GTQSLPTASASK	
Heat shock protein gp96 precursor	15010550	90.2	+ FAFQAEVNRMMK	
Hypothetical protein FLJ21820	11345458	37.3	+ DIYGLNGQIEHK	
Molecule possessing ankyrin repeats induced by lipopolysaccharide	38173790	78.1	+ CLIQMGAAVEAK	
Ubiquitin-conjugating enzyme E2G 2, isoform 1	15079469	18.6	+ RLMAEYK	
CGI-49 protein	7705767	46.9		+ AGGVFTPGAAFSK
DILV594	37182139	31.4		+ RELFSQIK
Hypothetical protein DKFZp564F0522.1—human (fragment)	7512734	33.1		+ ILRTSSGSIREK
Hypothetical protein HSPC117	7657015	55.2		+ EQLAQAMFDHIPVGVGSK
Tumor protein D52–like 2 isoform e	40805860	22.2		+ TQETLSQAGQK
Vesicle amine transport protein 1	15679945	41.9		+ VVTYGMANLLTGPK

[a]+, detected. [b]This peptide sequence is present in both Rab1A and Rab1B.

monoclonal anti-ADRP antibody (PROGEN Biotechnik GmbH, Heidelberg, Germany) (1:25), a guinea pig polyclonal anti-TIP47 antibody (PROGEN Biotechnik GmbH) (1:250), a mouse monoclonal anti-HCV core protein antibody (Anogen, Ontario, Canada) (1: 1,000), a mouse monoclonal anti-DDX1 antibody (Pharmingen, San Diego, CA, USA) (1:500), or a rabbit polyclonal anti-DDX3 antibody (antibody custom-made by Invitrogen, CA, USA) (1:500) for 90 min at room temperature. The blots were then incubated with horseradish peroxidase (HRP)–conjugated goat anti-rabbit IgG (BIO-RAD), HRP-conjugated goat anti-mouse IgG (BIO-RAD), or HRP-conjugated goat anti-guinea pig IgG (ICN Pharmaceuticals, Aurora, OH, USA) at 1:2,000 dilution for 60 min. Detection of immunoreactive proteins was performed with an ECL system (Amersham Biosciences Corp., Piscataway, NJ, USA).

RESULTS

Proteomic Analysis of Lipid Droplets by 1-D-SDS-PAGE/MALDI-TOF MS—Lipid droplet proteins from control (HCV core non-expressing) Hepswx cells and HCV core–expressing Hep39 cells were separated by 10% SDS-PAGE, and the protein bands were visualized by Coomassie Brilliant Blue staining (Fig. 2). In each cell line ~30 bands were seen. The visible bands (areas) were excised from the gels, trypsinized, and analyzed by MALDI-TOF MS. Among the 31 bands, we identified 25 proteins: 15 proteins in Hepswx cells and 23 proteins in Hep39 cells (Fig. 2 and Table 1). Thirteen of the 25 proteins were detected in both types of cell. The lipid droplet proteins found in both Hepswx and Hep39 cells could be categorized into four groups: (1) PAT family proteins, *i.e.* ADRP and TIP47; (2) multiple molecules involved in lipid metabolism; (3) several Rab GTPases; and (4) other/unknown proteins (Table 1). In addition, Hep39 cells contained another group of proteins involved in RNA metabolism/binding (Table 1).

Fig. 2. **Signature SDS-PAGE patterns of the lipid droplet fractions of Hepswx and Hep39 cells.** Proteins in the purified lipid droplet fractions (30 μg of protein per lane) of Hepswx cells and Hep39 cells were separated in a 10% SDS–polyacrylamide gel, and visualized by Coomassie Brilliant Blue staining. The 31 numbered bands were excised from the gel, subjected to in-gel trypsin digestion, and processed for MALDI-TOF-MS. Molecular weights (MW) are given to the left of the gel.

Proteomic Analysis of Lipid Droplets by DNLC-MS/MS—Some protein bands in Fig. 2 could not be identified, probably due to the restricted separation capacity of 1-D-SDS-PAGE (*i.e.* multiple proteins migrating to the same area). We had, however, difficulty in applying 2-DE to the separation of lipid droplet proteins because of their hydrophobic characteristics. We then tried a new LC-based MS strategy. Lipid droplet fractions from Hepswx and Hep39 cells were delipidated and then digested with Lys-C. The resulting peptide mixtures were directly analyzed using a DNLC-MS/MS system (*52*). We identified 36 lipid droplet proteins: 24 proteins in Hepswx cells and 27 proteins in Hep39 cells (Table 2). Twenty-three lipid droplet proteins were newly identified with this system. Fifteen proteins detected in both cell lines were classified into four categories (Table 2) as in the case of 1-D-SDS-PAGE/MALDI-TOF MS analysis. A group of proteins involved in RNA metabolism/binding was also found only in Hep39 cells (Table 2).

Proteins Exhibiting Differences in Their Association with Lipid Droplets Due to HCV Core Protein Expression—SDS-PAGE patterns of lipid droplet proteins were similar but revealed several distinct differences in protein composition between Hepswx and Hep39 cells (Fig. 2). The most remarkable differences were seen in the bands corresponding to PAT family proteins. The amount of ADRP, a major PAT family protein in lipid droplets in the liver (*54*, *55*), and likely to be the most abundant lipid droplet protein in Hepswx cells (Fig. 2, band 5), seemed to be less in HCV core–expressing Hep39 cells (Fig. 2, band 21). On the other hand, TIP47, which is also known to be a PAT family protein in lipid droplets (*56*, *57*), was detected as a major protein only in Hep39 cells (Fig. 2, band 22, and Table 1). To confirm these findings, the contents of ADRP and TIP47 in the lipid droplet fractions of Hepswx and Hep39 cells were examined by immunoblot analysis with specific antibodies. The lipid droplet fraction of HCV core–expressing Hep39 cells showed an apparently lower content of ADRP and a much higher content of TIP47 than the levels in Hepswx cells (Fig. 3).

Next we examined the cellular distributions of ADRP and TIP47 in Hepswx and Hep39 cells by cell fractionation. ADRP was highly concentrated in the lipid droplet fractions of both cells, even though the content in the lipid droplets was much lower in Hep39 cells than in Hepswx cells (Fig. 4). ADRP was not detected in post-nuclear supernatant fractions or in either the cytosol or membrane fractions, probably because of low expression levels in these cells or low affinity of the anti-ADRP antibody we used

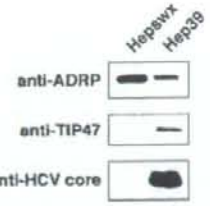

Fig. 3. **The lipid droplet fraction of Hep39 cells contains less ADRP, but more TIP47, than Hepswx cells.** Lipid droplet fractions (1.5 μg of protein per lane) from Hepswx and Hep39 cells were analyzed by immunoblotting with the indicated antibodies.

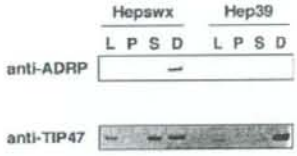

Fig. 4. **Subcellular localization of ADRP and TIP47 in Hepswx and Hep39 cells.** Hepswx and Hep39 cells were fractionated into post-nuclear supernatant (lane L), 100,000 × *g* precipitate (lane P), 100,000 × *g* supernatant (lane S), and lipid droplet (lane D) fractions as described in "MATERIALS AND METHODS." Ten micrograms of protein was processed for gel electrophoresis, and then analyzed by immunoblotting with anti-ADRP and anti-TIP47 antibodies.

(Fig. 4). The mRNA expression level of ADRP in Hep39 cells was less than half that in Hepswx cells (data not shown), consistent with the immunoblot data shown in Fig. 4. These results suggest that the lower ADRP content in the lipid droplet fraction of Hep39 cells is due to a low expression level of ADRP. In contrast, Hep39 cells had much more TIP47 in the lipid droplet fraction (Figs. 3 and 4, lanes D), but the cellular TIP47 content of Hep39 cells was not more than that in Hepswx cells (Fig. 4, lanes L). Besides the lipid droplet fraction, the cytosolic fraction of Hepswx cells was found to contain TIP47 at a substantial level, while the cytosolic fraction of Hep39 cells did not (Fig. 4, lanes S). These results indicate that the intracellular distribution of TIP47 shifts drastically from the cytosol to lipid droplets in HCV core–expressing Hep39 cells.

Another obvious difference between Hepswx and Hep39 cells in Fig. 2 is the presence of a specific ~85 kDa band (Fig. 2, band 16) in Hep39 cells, which was identified as DEAD box protein 1 (DDX1), a DEAD box protein family member, by 1-D-SDS-PAGE/MALDI-TOF MS analysis (Table 1). DNLC-MS/MS analysis also supported the existence of DDX1 in the lipid droplet fraction of Hep39 cells (Table 2). In addition, DEAD box protein 3 (DDX3), another DEAD box protein family member, was also detected in the lipid droplet fraction of Hep39 cells by means of the two different strategies used for proteomic analysis (Tables 1 and 2), suggesting that DDX3 is a major lipid droplet protein in Hep39 cells. To verify the association of DDX 1 and DDX3 with lipid droplets in Hep39 cells, immunoblot analysis was carried out. Figure 5 shows that DDX 1 and DDX 3 exist in the lipid droplet fraction of HCV core-expressing Hep39 cells, but not Hepswx cells. These results imply the special pathological functions of DDX1 and DDX3 in lipid droplets in HCV core–expressing cells.

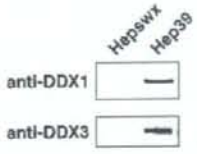

Fig. 5. **Hep39 cells, but not Hepswx cells, have DDX1 and DDX3 in the lipid droplet fraction.** Lipid droplet fractions (0.5 μg of protein per lane) in Hepswx and Hep39 cells were analyzed by immunoblotting with anti-DDX1 and anti-DDX3 antibodies.

DISCUSSION

To analyze lipid droplet proteins, we performed proteomic analysis by means of 1-D-SDS-PAGE/MALDI-TOF MS and automated DNLC-MS/MS, and identified 25 and 36 proteins, respectively (Tables 1 and 2). Many more lipid droplet proteins were identified by DNLC-MS/MS, and 22 major proteins separated by 1-D-SDS-PAGE (Fig. 2, bands, 2, 3, 4, 5, 7, 9, 10, 12, 13, 16, 17, 18, 21, 22, 24, 26, 27, 29, and 30) and detected on MALDI-TOF MS analysis were also detected on DNLC-MS/MS analysis. These results indicate that DNLC-MS/MS is a very sensitive and reliable system as well as a high-throughput method. Particularly, DNLC-MS/MS would be a powerful system for exhaustive proteomic analysis of protein mixtures/complexes (up to ~100 proteins) such as lipid droplets.

In our targeted proteomic study, we identified a total of 48 lipid droplet proteins: 30 proteins in control Hepswx cells, 38 proteins in HCV core–expressing Hep39 cells, and 20 proteins in both cell lines. The resident lipid droplet proteins were classified into four groups (Tables 1 and 2), consistent with the recently reported data obtained on proteomic analysis of lipid droplet proteins in other cell lines (*58–60*). In addition, multiple proteins, such as the sterol carrier protein 2–related form, fatty acid binding protein 5, and apoptosis-inducing factor homologous mitochondrion-associated inducer of death, were newly identified as lipid droplet proteins in this study. These accumulated data obtained on proteomic analysis will be useful for understanding the biogenesis and functions of lipid droplets about which little is yet known.

A prominent effect of the expression of HCV core protein on the composition of lipid droplet proteins was observed among the PAT family proteins, i.e. ADRP and TIP47. HCV core–expressing Hep39 cells contained much less ADRP in the lipid droplet fraction (Fig. 3), probably because of the lower cellular expression level and the lack of induction of expression upon lipid loading (data not shown). In contrast, a substantial amount of TIP47 was associated with the lipid droplet fraction of Hep39 cells (Fig. 3). Perilipin, a structural protein of lipid droplets in adipocytes, ADRP, and TIP47, termed PAT family proteins (*61*), share extensive amino acid sequence similarity (*61–63*), suggesting a common biological function in lipid droplet formation. For example, the transition in surface protein composition of lipid droplets from ADRP to perilipin occurs during adipocyte differentiation (*64*). Thus, TIP47 might replace ADRP

on the lipid droplets in Hep39 cells. Cellular TIP47 was not up-regulated in Hep39 cells, resulting in a reduction of TIP47 in the cytosolic fraction (Fig. 4). Since TIP47, originally identified as having the ability to interact with the mannose 6-phosphate/IGF-II receptor (*63*), appears to be essential for the endocytic recycling system (*65–67*), the altered distribution of cellular TIP47 in Hep39 cells could affect intracellular membrane trafficking pathways. Consistent with this assumption, our preliminary results showed that the rate of protein secretion from cells was apparently slower for Hep39 cells than Hepswx cells (unpublished data). Patients chronically infected with HCV (*68*) and HCV core–transgenic mice (*69*) exhibit decreased levels of plasma very low density lipoproteins secreted from the liver, also suggesting interference with intracellular membrane trafficking (secretion pathways) by HCV core proteins. We currently speculate that the reduction in cellular ADRP expression mediated by HCV core protein causes the accumulation of TIP47 in lipid droplets as a substitute, and that the resulting depletion of TIP47 in the cytosol could cause the impairment of intracellular membrane trafficking, followed by the cellular accumulation of membrane lipids and consequent lipid droplet formation. Although further studies remain to be done to confirm these possibilities, we suggest that HCV core protein influences not only the biogenesis of lipid droplets but also intracellular membrane trafficking.

Another interesting finding in this study is that Hep39 cells, unlike Hepswx cells, contain DEAD box proteins, DDX1 and DDX3, as major lipid droplet proteins (Figs. 2 and 5). On the basis of the results of studies involving yeast two-hybrid assays, DDX3 has been shown to be able to interact with HCV core protein, and studies involving immunofluorescent microscopy have revealed that DDX3 is distributed in cytosolic spots such as lipid droplets (*27, 70, 71*). These results, together with our present findings, suggest that DDX3 is associated with lipid droplets via HCV core proteins located on lipid droplets. In addition to DDX1 and DDX3, which possess ATPase/RNA helicase activities (*27, 72, 73*), several other proteins involved in RNA metabolism/binding, including HC56/gemin 4 and IGF-II mRNA–binding protein 3, were also detected in the lipid droplet fraction of HCV core-expressing Hep39 cells (Tables 1 and 2). Recently Dvorak *et al.* reported that RNA itself can be associated with lipid droplets in human mast cells (*74*). Taken together, these data strongly suggest that lipid droplets containing HCV core proteins may participate in the RNA metabolism of the host and/or HCV in HCV-infected cells. Furthermore, the findings that DDX1 is overexpressed in cell lines derived from tumors such as retinoblastomas and neuroblastomas (*75*), and that cellular expression of DDX3 induces anchorage-independent cell growth (*76*) suggest the involvement of DDX1 and DDX3 in carcinogenesis.

Some groups recently reported profiles of mRNAs up- or down-regulated by expression of the HCV core protein (*77–79*), but these mRNAs included no molecules identified as lipid droplet proteins in this study. Since lipid droplets are a minor organelle in cells, it might be difficult to detect changes in the mRNA expression levels of lipid droplet proteins. The merits of targeted proteomic study are that it is possible to focus on minor cellular fractions, and also to detect changes in the intracellular distributions of proteins. Actually, the mRNA expression levels of TIP47, DDX1, and DDX3 did not change in Hep39 cells (data not shown).

We identified many other lipid droplet proteins found in either Hepswx or Hep39 cells, but their biological functions remain mostly unknown (Tables 1 and 2). Elucidation of the biological functions of these proteins will lead to an advanced understanding of the pathogeneses of HCV-derived liver diseases.

This work was supported by Grants-in-Aid from the Ministry of Health, Labor and Welfare; the program for the Promotion of Fundamental Studies in Health Sciences of the Organization for Drug ADR Relief, R&D Promotion, and Product Review of Japan; the TAKEDA SCIENCE FOUNDATION; and the Integrated Proteomics System Project for Pioneer Research on Genome the Frontier from the Ministry of Education, Culture, Sports, Science & Technology of Japan.

REFERENCES

1. Choo, Q.L., Kuo, G., Weiner, A.J., Overby, L.R., Bradley, D.W., and Houghton, M. (1989) Isolation of a cDNA clone derived from a blood-borne non-A, non-B viral hepatitis genome. *Science* **244**, 359–362
2. Kuo, G., Choo, Q.L., Alter, H.J., Gitnick, G.L., Redeker, A.G., Purcell, R.H., Miyamura, T., Dienstag, J.L., Alter, M.J., Stevens, C.E., Tegtmeier, G.E., Bonino, F., Colombo, M., Lee, W.-S., Kuo, C., Berger, K., Shuster, J.R., Overby, L.R., Bradley, D.W., and Houghton, M. (1989) An assay for circulating antibodies to a major etiologic virus of human non-A, non-B hepatitis. *Science* **244**, 362–364
3. Saito, I., Miyamura, T., Ohbayashi, A., Harada, H., Katayama, T., Kikuchi, S., Watanabe, Y., Koi, S., Onji, M., Ohta, Y., Choo, Q.-L., Houghton, M., and Kuo, G. (1990) Hepatitis C virus infection is associated with the development of hepatocellular carcinoma. *Proc. Natl. Acad. Sci. USA* **87**, 6547–6549
4. Kiyosawa, K., Sodeyama, T., Tanaka, E., Gibo, Y., Yoshizawa, K., Nakano, Y., Furuta, S., Akahane, Y., Nishioka, K., Purcell, R.H., and Alter, H.J. (1990) Interrelationship of blood transfusion, non-A, non-B hepatitis and hepatocellular carcinoma: analysis by detection of antibody to hepatitis C virus. *Hepatology* **12**, 671–675
5. Bartenschlager, R. and Lohmann, V. (2000) Replication of hepatitis C virus. *J. Gen. Virol.* **81**, 1631–1648
6. Grakoui, A., Wychowski, C., Lin, C., Feinstone, S.M., and Rice, C.M. (1993) Expression and identification of hepatitis C virus polyprotein cleavage products. *J. Virol.* **67**, 1385–1395
7. McLauchlan, J., Lemberg, M.K., Hope, G., and Martoglio, B. (2002) Intramembrane proteolysis promotes trafficking of hepatitis C virus core protein to lipid droplets. *EMBO J.* **21**, 3980–3988
8. Okamoto, K., Moriishi, K., Miyamura, T., and Matsuura, Y. (2004) Intramembrane proteolysis and endoplasmic reticulum retention of hepatitis C virus core protein. *J. Virol.* **78**, 6370–6380
9. Santolini, E., Migliaccio, G., and La Monica, N. (1994) Biosynthesis and biochemical properties of the hepatitis C virus core protein. *J. Virol.* **68**, 3631–3641
10. Barba, G., Harper, F., Harada, T., Kohara, M., Goulinet, S., Matsuura, Y., Eder, G., Schaff, Z., Chapman, M.J., Miyamura, T., and Brechot, C. (1997) Hepatitis C virus core protein shows a cytoplasmic localization and associates to cellular lipid storage droplets. *Proc. Natl. Acad. Sci. USA* **94**, 1200–1205
11. Ray, R.B., Lagging, L.M., Meyer, K., and Ray, R. (1996) Hepatitis C virus core protein cooperates with ras and transforms

primary rat embryo fibroblasts to tumorigenic phenotype. *J. Virol.* **70**, 4438–4443
12. Yoshida, T., Hanada, T., Tokuhisa, T., Kosai, K., Sata, M., Kohara, M., and Yoshimura, A. (2002) Activation of STAT3 by the hepatitis C virus core protein leads to cellular transformation. *J. Exp. Med.* **196**, 641–653
13. Moriya, K., Yotsuyanagi, H., Shintani, Y., Fujie, H., Ishibashi, K., Matsuura, Y., Miyamura, T., and Koike, K. (1997) Hepatitis C virus core protein induces hepatic steatosis in transgenic mice. *J. Gen. Virol.* **78**, 1527–1531
14. Moriya, K., Fujie, H., Shintani, Y., Yotsuyanagi, H., Tsutsumi, T., Ishibashi, K., Matsuura, Y., Kimura, S., Miyamura, T., and Koike, K. (1998) The core protein of hepatitis C virus induces hepatocellular carcinoma in transgenic mice. *Nat. Med.* **4**, 1065–1067
15. Kim, D.W., Suzuki, R., Harada, T., Saito, I., and Miyamura, T. (1994) Trans-suppression of gene expression by hepatitis C viral core protein. *Jpn. J. Med. Sci. Biol.* **47**, 211–220
16. Ray, R.B., Steele, R., Meyer, K., and Ray, R. (1997) Transcriptional repression of p53 promoter by hepatitis C virus core protein. *J. Biol. Chem.* **272**, 10983–10986
17. Shrivastava, A., Manna, S.K., Ray, R., and Aggarwal, B.B. (1998) Ectopic expression of hepatitis C virus core protein differentially regulates nuclear transcription factors. *J. Virol.* **72**, 9722–9728
18. Chen, C.M., You, L.R., Hwang, L.H., and Lee, Y.H. (1997) Direct interaction of hepatitis C virus core protein with the cellular lymphotoxin-beta receptor modulates the signal pathway of the lymphotoxin-beta receptor. *J. Virol.* **71**, 9417–9426
19. Zhu, N., Khoshnan, A., Schneider, R., Matsumoto, M., Dennert, G., Ware, C., and Lai, M.M. (1998) Hepatitis C virus core protein binds to the cytoplasmic domain of tumor necrosis factor (TNF) receptor 1 and enhances TNF-induced apoptosis. *J. Virol.* **72**, 3691–3697
20. Tsuchihara, K., Hijikata, M., Fukuda, K., Kuroki, T., Yamamoto, N., and Shimotohno, K. (1999) Hepatitis C virus core protein regulates cell growth and signal transduction pathway transmitting growth stimuli. *Virology* **258**, 100–107
21. You, L.R., Chen, C.M., and Lee, Y.H. (1999) Hepatitis C virus core protein enhances NF-kappaB signal pathway triggering by lymphotoxin-beta receptor ligand and tumor necrosis factor alpha. *J. Virol.* **73**, 1672–1681
22. Aoki, H., Hayashi, J., Moriyama, M., Arakawa, Y., and Hino, O. (2000) Hepatitis C virus core protein interacts with 14-3-3 protein and activates the kinase Raf-1. *J. Virol.* **74**, 1736–1741
23. Yoshida, H., Kato, N., Shiratori, Y., Otsuka, M., Maeda, S., Kato, J., and Omata, M. (2001) Hepatitis C virus core protein activates nuclear factor kappa B-dependent signaling through tumor necrosis factor receptor-associated factor. *J. Biol. Chem.* **276**, 16399–16405
24. Matsumoto, M., Hsieh, T.Y., Zhu, N., VanArsdale, T., Hwang, S.B., Jeng, K.S., Gorbalenya, A.E., Lo, S.Y., Ou, J.H., Ware, C.F., and Lai, M.M. (1997) Hepatitis C virus core protein interacts with the cytoplasmic tail of lymphotoxin-beta receptor. *J. Virol.* **71**, 1301–1309
25. Hsieh, T.Y., Matsumoto, M., Chou, H.C., Schneider, R., Hwang, S.B., Lee, A.S., and Lai, M.M. (1998) Hepatitis C virus core protein interacts with heterogeneous nuclear ribonucleoprotein K. *J. Biol. Chem.* **273**, 17651–17659
26. Sabile, A., Perlemuter, G., Bono, F., Kohara, K., Demaugre, F., Kohara, M., Matsuura, Y., Miyamura, T., Brechot, C., and Barba, G. (1999) Hepatitis C virus core protein binds to apolipoprotein AII and its secretion is modulated by fibrates. *Hepatology* **30**, 1064–1076
27. You, L.R., Chen, C.M., Yeh, T.S., Tsai, T.Y., Mai, R.T., Lin, C.H., and Lee, Y.H. (1999) Hepatitis C virus core protein interacts with cellular putative RNA helicase. *J. Virol.* **73**, 2841–2853
28. Jin, D.Y., Wang, H.L., Zhou, Y., Chun, A.C., Kibler, K.V., Hou, Y.D., Kung, H., and Jeang, K.T. (2000) Hepatitis C virus core protein-induced loss of LZIP function correlates with cellular transformation. *EMBO J.* **19**, 729–740
29. Wang, F., Yoshida, I., Takamatsu, M., Ishido, S., Fujita, T., Oka, K., and Hotta, H. (2000) Complex formation between hepatitis C virus core protein and p21Waf1/Cip1/Sdi1. *Biochem. Biophys. Res. Commun.* **273**, 479–484
30. Otsuka, M., Kato, N., Lan, K., Yoshida, H., Kato, J., Goto, T., Shiratori, Y., and Omata, M. (2000) Hepatitis C virus core protein enhances p53 function through augmentation of DNA binding affinity and transcriptional ability. *J. Biol. Chem.* **275**, 34122–34130
31. Tsutsumi, T., Suzuki, T., Shimoike, T., Suzuki, R., Moriya, K., Shintani, Y., Fujie, H., Matsuura, Y., Koike, K., and Miyamura, T. (2002) Interaction of hepatitis C virus core protein with retinoid X receptor alpha modulates its transcriptional activity. *Hepatology* **35**, 937–946
32. Hosui, A., Ohkawa, K., Ishida, H., Sato, A., Nakanishi, F., Ueda, K., Takehara, T., Kasahara, A., Sasaki, Y., Hori, M., and Hayashi, N. (2003) Hepatitis C virus core protein differently regulates the JAK-STAT signaling pathway under interleukin-6 and interferon-gamma stimuli. *J. Biol. Chem.* **278**, 28562–28571
33. Ohkawa, K., Ishida, H., Nakanishi, F., Hosui, A., Ueda, K., Takehara, T., Hori, M., and Hayashi, N. (2004) Hepatitis C virus core functions as a suppressor of cyclin-dependent kinase-activating kinase and impairs cell cycle progression. *J. Biol. Chem.* **279**, 11719–11726
34. Alisi, A., Giambartolomei, S., Cupelli, F., Merlo, P., Fontemaggi, G., Spaziani, A., and Balsano, C. (2003) Physical and functional interaction between HCV core protein and the different p73 isoforms. *Oncogene* **22**, 2573–2580
35. Okabe, H., Satoh, S., Kato, T., Kitahara, O., Yanagawa, R., Yamaoka, Y., Tsunoda, T., Furukawa, Y., and Nakamura, Y. (2001) Genome-wide analysis of gene expression in human hepatocellular carcinomas using cDNA microarray: identification of genes involved in viral carcinogenesis and tumor progression. *Cancer Res.* **61**, 2129–2137
36. Shirota, Y., Kaneko, S., Honda, M., Kawai, H.F., and Kobayashi, K. (2001) Identification of differentially expressed genes in hepatocellular carcinoma with cDNA microarrays. *Hepatology* **33**, 832–840
37. Iizuka, N., Oka, M., Yamada-Okabe, H., Mori, N., Tamesa, T., Okada, T., Takemoto, N., Tangoku, A., Hamada, K., Nakayama, H., Miyamoto, T., Uchimura, S., and Hamamoto, Y. (2002) Comparison of gene expression profiles between hepatitis B virus- and hepatitis C virus-infected hepatocellular carcinoma by oligonucleotide microarray data on the basis of a supervised learning method. *Cancer Res.* **62**, 3939–3944
38. Iizuka, N., Oka, M., Yamada-Okabe, H., Mori, N., Tamesa, T., Okada, T., Takemoto, N., Hashimoto, K., Tangoku, A., Hamada, K., Nakayama, H., Miyamoto, T., Uchimura, S., and Hamamoto, Y. (2003) Differential gene expression in distinct virologic types of hepatocellular carcinoma: association with liver cirrhosis. *Oncogene* **22**, 3007–3014
39. Smith, M.W., Yue, Z.N., Geiss, G.K., Sadovnikova, N.Y., Carter, V.S., Boix, L., Lazaro, C.A., Rosenberg, G.B., Bumgarner, R.E., Fausto, N., Bruix, J., and Katze, M.G. (2003) Identification of novel tumor markers in hepatitis C virus-associated hepatocellular carcinoma. *Cancer Res.* **63**, 859–864
40. Smith, M.W., Yue, Z.N., Korth, M.J., Do, H.A., Boix, L., Fausto, N., Bruix, J., Carithers, R.L., Jr., and Katze, M.G. (2003) Hepatitis C virus and liver disease: global transcriptional profiling and identification of potential markers. *Hepatology* **38**, 1458–1467
41. Takashima, M., Kuramitsu, Y., Yokoyama, Y., Iizuka, N., Toda, T., Sakaida, I., Okita, K., Oka, M., and Nakamura, K. (2003) Proteomic profiling of heat shock protein 70 family members as biomarkers for hepatitis C virus-related hepatocellular carcinoma. *Proteomics* **3**, 2487–2493

42. Yokoyama, Y., Kuramitsu, Y., Takashima, M., Iizuka, N., Toda, T., Terai, S., Sakaida, I., Oka, M., Nakamura, K., and Okita, K. (2004) Proteomic profiling of proteins decreased in hepatocellular carcinoma from patients infected with hepatitis C virus. *Proteomics* **4**, 2111–2116
43. Moradpour, D., Englert, C., Wakita, T., and Wands, J.R. (1996) Characterization of cell lines allowing tightly regulated expression of hepatitis C virus core protein. *Virology* **222**, 51–63
44. Hope, R.G. and McLauchlan, J. (2000) Sequence motifs required for lipid droplet association and protein stability are unique to the hepatitis C virus core protein. *J. Gen. Virol.* **81**, 1913–1925
45. Hope, R.G., Murphy, D.J., and McLauchlan, J. (2002) The domains required to direct core proteins of hepatitis C virus and GB virus-B to lipid droplets share common features with plant oleosin proteins. *J. Biol. Chem.* **277**, 4261–4270
46. Shi, S.T., Polyak, S.J., Tu, H., Taylor, D.R., Gretch, D.R., and Lai, M.M. (2002) Hepatitis C virus NS5A colocalizes with the core protein on lipid droplets and interacts with apolipoproteins. *Virology* **292**, 198–210
47. Harada, T., Kim, D.W., Sagawa, K., Suzuki, T., Takahashi, K., Saito, I., Matsuura, Y., and Miyamura, T. (1995) Characterization of an established human hepatoma cell line constitutively expressing non-structural proteins of hepatitis C virus by transfection of viral cDNA. *J. Gen. Virol.* **76**, 1215–1221
48. Balch, W.E. and Rothman, J.E. (1985) Characterization of protein transport between successive compartments of the Golgi apparatus: asymmetric properties of donor and acceptor activities in a cell-free system. *Arch. Biochem. Biophys.* **240**, 413–425
49. Yanagida, M., Miura, Y., Yagasaki, K., Taoka, M., Isobe, T., and Takahashi, N. (2000) Matrix assisted laser desorption/ionization-time of flight-mass spectrometry analysis of proteins detected by anti-phosphotyrosine antibody on two-dimensional-gels of fibrolast cell lysates after tumor necrosis factor-alpha stimulation. *Electrophoresis* **21**, 1890–1898
50. Yanagida, M., Shimamoto, A., Nishikawa, K., Furuichi, Y., Isobe, T., and Takahashi, N. (2001) Isolation and proteomic characterization of the major proteins of the nucleolin-binding ribonucleoprotein complexes. *Proteomics* **1**, 1390–1404
51. Bligh, E.G. and Dyer, W.J. (1959) A rapid method of total lipid extraction and purification. *Can. J. Med. Sci.* **37**, 911–917
52. Natsume, T., Yamauchi, Y., Nakayama, H., Shinkawa, T., Yanagida, M., Takahashi, N., and Isobe, T. (2002) A direct nanoflow liquid chromatography-tandem mass spectrometry system for interaction proteomics. *Anal. Chem.* **74**, 4725–4733
53. Yanagida, M., Hayano, T., Yamauchi, Y., Shinkawa, T., Natsume, T., Isobe, T., and Takahashi, N. (2004) Human fibrillarin forms a sub-complex with splicing factor 2-associated p32, protein arginine methyltransferases, and tubulins alpha 3 and beta 1 that is independent of its association with preribosomal ribonucleoprotein complexes. *J. Biol. Chem.* **279**, 1607–1614
54. Heid, H.W., Moll, R., Schwetlick, I., Rackwitz, H.R., and Keenan, T.W. (1998) Adipophilin is a specific marker of lipid accumulation in diverse cell types and diseases. *Cell Tissue Res.* **294**, 309–321
55. Londos, C., Brasaemle, D.L., Schultz, C.J., Segrest, J.P., and Kimmel, A.R. (1999) Perilipins, ADRP, and other proteins that associate with intracellular neutral lipid droplets in animal cells. *Semin. Cell Dev. Biol.* **10**, 51–58
56. Wolins, N.E., Rubin, B. and Brasaemle, D.L. (2001) TIP47 associates with lipid droplets. *J. Biol. Chem.* **276**, 5101–5108
57. Miura, S., Gan, J.W., Brzostowski, J., Parisi, M.J., Schultz, C.J., Londos, C., Oliver, B., and Kimmel, A.R. (2002) Functional conservation for lipid storage droplet association among Perilipin, ADRP, and TIP47 (PAT)-related proteins in mammals, Drosophila, and Dictyostelium. *J. Biol. Chem.* **277**, 32253–32257
58. Liu, P., Ying, Y., Zhao, Y., Mundy, D.I., Zhu, M., and Anderson, R.G. (2004) Chinese hamster ovary K2 cell lipid droplets appear to be metabolic organelles involved in membrane traffic. *J. Biol. Chem.* **279**, 3787–3792
59. Fujimoto, Y., Itabe, H., Sakai, J., Makita, M., Noda, J., Mori, M., Higashi, Y., Kojima, S., and Takano, T. (2004) Identification of major proteins in the lipid droplet-enriched fraction isolated from the human hepatocyte cell line HuH7. *Biochim. Biophys. Acta* **1644**, 47–59
60. Brasaemle, D.L., Dolios, G., Shapiro, L., and Wang, R. (2004) Proteomic analysis of proteins associated with lipid droplets of basal and lipolytically stimulated 3T3-L1 adipocytes. *J. Biol. Chem.* **279**, 46835–46842
61. Lu, X., Gruia-Gray, J., Copeland, N.G., Gilbert, D.J., Jenkins, N.A., Londos, C., and Kimmel, A.R. (2001) The murine perilipin gene: the lipid droplet-associated perilipins derive from tissue-specific, mRNA splice variants and define a gene family of ancient origin. *Mamm. Genome* **12**, 741–749
62. Greenberg, A.S., Egan, J.J., Wek, S.A., Moos, M.C., Jr., Londos, C., and Kimmel, A.R. (1993) Isolation of cDNAs for perilipins A and B: sequence and expression of lipid droplet-associated proteins of adipocytes. *Proc. Natl. Acad. Sci. USA* **90**, 12035–12039
63. Diaz, E. and Pfeffer, S.R. (1998) TIP47: a cargo selection device for mannose 6-phosphate receptor trafficking. *Cell* **93**, 433–443
64. Brasaemle, D.L., Barber, T., Wolins, N.E., Serrero, G., Blanchette-Mackie, E.J., and Londos, C. (1997) Adipose differentiation-related protein is an ubiquitously expressed lipid storage droplet-associated protein. *J. Lipid Res.* **38**, 2249–2263
65. Carroll, K.S., Hanna, J., Simon, I., Krise, J., Barbero, P., and Pfeffer, S.R. (2001) Role of Rab9 GTPase in facilitating receptor recruitment by TIP47. *Science* **292**, 1373–1376
66. Pfeffer, S.R. (2001) Rab GTPases: specifying and deciphering organelle identity and function. *Trends Cell Biol.* **11**, 487–491
67. Blot, G., Janvier, K., Le Panse, S., Benarous, R., and Berlioz-Torrent, C. (2003) Targeting of the human immunodeficiency virus type 1 envelope to the trans-Golgi network through binding to TIP47 is required for env incorporation into virions and infectivity. *J. Virol.* **77**, 6931–6945
68. Serfaty, L., Andreani, T., Giral, P., Carbonell, N., Chazouilleres, O., and Poupon, R. (2001) Hepatitis C virus induced hypobetalipoproteinemia: a possible mechanism for steatosis in chronic hepatitis C. *J. Hepatol.* **34**, 428–434
69. Perlemuter, G., Sabile, A., Letteron, P., Vona, G., Topilco, A., Chretien, Y., Koike, K., Pessayre, D., Chapman, J., Barba, G., and Brechot, C. (2002) Hepatitis C virus core protein inhibits microsomal triglyceride transfer protein activity and very low density lipoprotein secretion: a model of viral-related steatosis. *FASEB J.* **16**, 185–194
70. Owsianka, A.M. and Patel, A.H. (1999) Hepatitis C virus core protein interacts with a human DEAD box protein DDX3. *Virology* **257**, 330–340
71. Mamiya, N. and Worman, H.J. (1999) Hepatitis C virus core protein binds to a DEAD box RNA helicase. *J. Biol. Chem.* **274**, 15751–15756
72. Gururajan, R. and Weeks, D.L. (1997) An3 protein encoded by a localized maternal mRNA in Xenopus laevis is an ATPase with substrate-specific RNA helicase activity. *Biochim. Biophys. Acta* **1350**, 169–182
73. Chen, H.C., Lin, W.C., Tsay, Y.G., Lee, S.C., and Chang, C.J. (2002) An RNA helicase, DDX1, interacting with poly(A) RNA and heterogeneous nuclear ribonucleoprotein K. *J. Biol. Chem.* **277**, 40403–40409
74. Dvorak, A.M., Morgan, E.S., and Weller, P.F. (2003) RNA is closely associated with human mast cell lipid bodies. *Histol. Histopathol.* **18**, 943–968
75. Godbout, R., Packer, M., and Bie, W. (1998) Overexpression of a DEAD box protein (DDX1) in neuroblastoma and retinoblastoma cell lines. *J. Biol. Chem.* **273**, 21161–21168

76. Huang, J.S., Chao, C.C., Su, T.L., Yeh, S.H., Chen, D.S., Chen, C.T., Chen, P.J., and Jou, Y.S. (2004) Diverse cellular transformation capability of overexpressed genes in human hepatocellular carcinoma. *Biochem. Biophys. Res. Commun.* **315**, 950–958
77. Liu, M., Liu, Y., Cheng, J., Zhang, S.L., Wang, L., Shao, Q., Zhang, J., and Yang, Q. (2004) Transactivating effect of hepatitis C virus core protein: a suppression subtractive hybridization study. *World J. Gastroenterol.* **10**, 1746–1749
78. Ohkawa, K., Ishida, H., Nakanishi, F., Hosui, A., Sato, A., Ueda, K., Takehara, T., Kasahara, A., Sasaki, Y., Hori, M., and Hayashi, N. (2003) Changes in gene expression profile by HCV core protein in cultured liver cells: analysis by DNA array assay. *Hepatol. Res.* **25**, 396–408
79. Sacco, R., Tsutsumi, T., Suzuki, R., Otsuka, M., Aizaki, H., Sakamoto, S., Matsuda, M., Seki, N., Matsuura, Y., Miyamura, T., and Suzuki, T. (2003) Antiapoptotic regulation by hepatitis C virus core protein through up-regulation of inhibitor of caspase-activated DNase. *Virology* **317**, 24–35

JOURNAL OF VIROLOGY, Feb. 2007, p. 1174–1185
0022-538X/07/$08.00+0 doi:10.1128/JVI.01684-06

Vol. 81, No. 3

E6AP Ubiquitin Ligase Mediates Ubiquitylation and Degradation of Hepatitis C Virus Core Protein▽

Masayuki Shirakura,[1] Kyoko Murakami,[1] Tohru Ichimura,[2] Ryosuke Suzuki,[1] Tetsu Shimoji,[1] Kouichirou Fukuda,[1] Katsutoshi Abe,[1] Shigeko Sato,[3] Masayoshi Fukasawa,[3] Yoshio Yamakawa,[3] Masahiro Nishijima,[3] Kohji Moriishi,[4] Yoshiharu Matsuura,[4] Takaji Wakita,[1] Tetsuro Suzuki,[1] Peter M. Howley,[5] Tatsuo Miyamura,[1] and Ikuo Shoji[1]*

Department of Virology II[1] and Department of Biochemistry and Cell Biology,[3] National Institute of Infectious Diseases, Shinjuku-ku, Tokyo 162-8640, Japan; Department of Chemistry, Graduate School of Science, Tokyo Metropolitan University, Hachioji-shi, Tokyo 192-0397, Japan[2]; Department of Molecular Virology, Research Institute for Microbial Diseases, Osaka University, Osaka 565-0871, Japan[4]; and Department of Pathology, Harvard Medical School, 77 Avenue Louis Pasteur, Boston, Massachusetts 02115[5]

Received 4 August 2006/Accepted 8 November 2006

Hepatitis C virus (HCV) core protein is a major component of viral nucleocapsid and a multifunctional protein involved in viral pathogenesis and hepatocarcinogenesis. We previously showed that the HCV core protein is degraded through the ubiquitin-proteasome pathway. However, the molecular machinery for core ubiquitylation is unknown. Using tandem affinity purification, we identified the ubiquitin ligase E6AP as an HCV core-binding protein. E6AP was found to bind to the core protein in vitro and in vivo and promote its degradation in hepatic and nonhepatic cells. Knockdown of endogenous E6AP by RNA interference increased the HCV core protein level. In vitro and in vivo ubiquitylation assays showed that E6AP promotes ubiquitylation of the core protein. Exogenous expression of E6AP decreased intracellular core protein levels and supernatant HCV infectivity titers in the HCV JFH1-infected Huh-7 cells. Furthermore, knockdown of endogenous E6AP by RNA interference increased intracellular core protein levels and supernatant HCV infectivity titers in the HCV JFH1-infected cells. Taken together, our results provide evidence that E6AP mediates ubiquitylation and degradation of HCV core protein. We propose that the E6AP-mediated ubiquitin-proteasome pathway may affect the production of HCV particles through controlling the amounts of viral nucleocapsid protein.

Hepatitis C virus (HCV; a single-stranded, positive-sense RNA virus that is classified in the family *Flaviviridae*) is the main cause of chronic hepatitis, liver cirrhosis, and hepatocellular carcinoma (5, 26, 45). More than 170 million people worldwide are chronically infected with HCV (41). The approximately 9.6-kb HCV genome encodes a unique open reading frame that is translated into a polyprotein (5, 54). The polyprotein is cleaved cotranslationally into at least 10 proteins by viral proteases and cellular signalases (6, 10).

The HCV core protein represents the first 1 to 191 amino acids (aa) of the polyprotein and is followed by two glycoproteins, E1 and E2 (6). The core protein plays a central role in the packaging of viral RNA (25, 40); modulates various cellular processes, including signal transduction pathways, transcriptional control, cell cycle progression, apoptosis, lipid metabolism, and the immune response (9, 40); and has transforming potential in certain cells (43). Mice transgenic for the HCV core gene develop steatosis (32) and later hepatocellular carcinoma (31). These findings suggest that HCV core protein plays a crucial role in hepatocarcinogenesis.

Two major forms of the HCV core protein, p21 (mature form) and p23 (immature form), can be generated in cultured cells (60). Cellular signal peptidase cleaves at the junction of the core/E1, releasing the immature form of the core protein from the polypeptide (12, 46). Signal peptide peptidase cleaves just before the signal sequence, liberating the mature form of the HCV core protein at the cytoplasmic face of the endoplasmic reticulum (29). Several different sites have been proposed as potential cleavage sites of signal peptide peptidase, such as Leu-179 (15, 29), Phe-177 (36, 37), Leu-182 (15), and Ser-173 (46). Further processing of the HCV core protein yields a 17-kDa product with a C terminus at around amino acid 152. A truncated form of the core protein, p17, was found in transfected cells (42, 52) and liver tissues from humans with hepatocellular carcinoma (59). The majority of this protein translocates to the nucleus. The C terminus of the core protein is important for regulating the stability of the protein (20, 52).

We previously showed that the C-terminally truncated forms of the core protein are degraded through the ubiquitin-proteasome pathway (52). We found that the mature form of the core protein, p21, also links to a few ubiquitin moieties, suggesting that the ubiquitin-proteasome pathway involves proteolysis of heterologous species of the core protein (52). Overexpression of PA28γ (a REG family proteasome activator also known as REGγ or Ki antigen) enhances the proteasomal degradation of the HCV core protein (30). A recent study has shown that

* Corresponding author. Mailing address: Department of Virology II, National Institute of Infectious Diseases, 1-23-1 Toyama, Shinjuku-ku, Tokyo 162-8640, Japan. Phone: 81 3-5285-1111. Fax: 81 3-5285-1161. E-mail: ishoji@nih.go.jp.

▽ Published ahead of print on 15 November 2006.

PA28γ is involved in the degradation of the steroid receptor coactivator 3 (SRC-3) in an ATP- and ubiquitin-independent manner (27). It is still unclear what E3 ubiquitin ligase is responsible for ubiquitylation of the HCV core protein.

E6AP was initially identified as the cellular factor that stimulates ubiquitin-mediated degradation of the tumor suppressor p53 in conjunction with the E6 protein of cancer-associated human papillomavirus types 16 and 18 (14, 48). The E6-E6AP complex functions as a E3 ubiquitin ligase in the ubiquitylation of p53 (49). E6AP is the prototype of a family of ubiquitin ligases called HECT domain ubiquitin ligases, all of which contain a domain *h*omologous to the *E6AP c*arboxyl *t*erminus (13). Interestingly, E6AP is not involved in the regulation of p53 ubiquitylation in the absence of E6 (55). Several potential E6-independent substrates for E6AP have been identified, such as hHR23A, Blk, and Mcm7 (23, 24, 35). E6AP is also a candidate gene for Angelman syndrome, which is a severe neurological disorder characterized by mental retardation (21).

This study aimed to identify endogenous ubiquitin-proteasome pathway proteins that are associated with HCV core protein. Tandem affinity purification and mass spectrometry analysis identified E6AP as an HCV core-binding protein. Here we present evidence that E6AP associates with HCV core protein in vitro and in vivo and is involved in ubiquitylation and degradation of HCV core protein. We propose that an E6AP-mediated ubiquitin-proteasome pathway may affect the production of HCV particles through controlling the amounts of HCV core protein.

MATERIALS AND METHODS

Cell culture and transfection. Human embryonic kidney 293T cells, human hepatoblastoma HepG2 cells, and human hepatoma Huh-7 cells were cultured in Dulbecco's modified Eagle's medium (Sigma) supplemented with 50 IU/ml penicillin, 50 μg/ml streptomycin (Invitrogen), and 10% (vol/vol) fetal bovine serum (JRH Biosciences) at 37°C in a 5% CO_2 incubator. 293T cells and HepG2 cells were transfected with plasmid DNA using FuGene 6 transfection reagents (Roche). Huh-7 cells were transfected with plasmid DNA using *Trans*IT LT1 transfection reagents (Mirus).

Plasmids and recombinant baculoviruses. MEF tag cassette (containing *myc* tag, the tobacco etch virus protease cleavage site, and *F*LAG tag) (16) was fused to the N terminus of the cDNA encoding core protein of HCV NIHJ1 (genotype 1b) (1). To express MEF-tagged core protein in mammalian cells, the genome coding for HCV core protein (amino acids 1 to 191) was amplified by PCR using pBR HCV NIHJ1 as a template. Sense oligonucleotide containing a Kozak consensus translation initiation codon and antisense oligonucleotide containing an in-frame translation stop codon were synthesized by PCR. The amplified PCR product was purified, digested with EcoRI and EcoRV, and then inserted into the EcoRI-EcoRV site of pcDNA3-MEF. FLAG-tagged HCV core expression plasmids based upon pCAGGS (34) were described previously (30). To express E6AP and the active-site cysteine-to-alanine mutant of E6AP in mammalian cells, pCMV4-HA-E6AP isoform II and pCMV4-HA-E6AP C-A were utilized (19). The C-A mutation was introduced at the site of E6AP C843. To express E6AP and E6AP C-A under the CAG promoter, the E6AP fragment and the E6AP C-A fragment were amplified by PCR, purified, digested with SmaI and NotI, and blunt ended using a DNA blunting kit (Takara). These PCR fragments were subcloned into pCAGGS.

To make a fusion protein consisting of glutathione *S*-transferase (GST) fused to the N terminus of E6AP in *Escherichia coli*, the E6AP fragment was amplified by PCR and the resultant product was cloned into the SmaI-NotI site of pGEX4T-1 vector (Amersham Biosciences). To express a series of E6AP truncation mutants as GST fusion proteins, each fragment was amplified by PCR and cloned into the SmaI-NotI site of pGEX4T-1. To purify GST core protein efficiently by two-step affinity purification, we fused hexahistidine (His) tag to the C terminus of GST fusion proteins. To bacterially express HCV core (aa 1 to 173) protein as a fusion protein containing N-terminal GST tag and C-terminal His tag, core fragment was amplified by PCR and the resultant product was cloned into the EcoRI-NotI site of pGEX4T-1 vector. The resultant plasmid was designated pGEX GST-C173HT. To express GST core (1–152)-His and GST-His in *E. coli*, pGEX core (1–152)-His and pGEX-His were constructed similarly. The resultant plasmids were designated pGEX GST-C152HT and pGEX GST-HT, respectively.

To generate recombinant baculoviruses expressing GST-E6AP, GST-E6AP fragment was excised from pGEX E6AP by digestion with SmaI and Tth111I and ligated into the SmaI-Tth111I site of pVL1392 (Invitrogen). To express GST-E6AP C-A, pVLGST-E6AP C-A was constructed similarly. To generate recombinant baculovirus expressing HCV core (aa 1 to 173) protein as a fusion protein containing N-terminal GST tag and C-terminal His tag, GST-C173HT fragment was amplified by PCR using pGEX GST-C173HT as a template, digested with BglII-XbaI, and subcloned into the BglII-XbaI site of pVL1392. To generate recombinant baculoviruses expressing GST-C152HT and GST-HT, cDNA fragments corresponding to GST-C152HT and GST-HT were amplified by PCR and subcloned into pVL1392, respectively. The resultant plasmids were designated pVLGST-C173HT, pVLGST-C152HT, and pVLGST-HT. To generate recombinant baculovirus expressing MEF-tagged E6AP, cDNA fragment encoding MEF-E6AP was subcloned into pVL1392. To express HCV core protein in the TNT-coupled wheat germ lysate system (Promega), HCV core cDNA was inserted in the EcoRI site of pCMVTNT (Promega). The primer sequences used in this study are available from the authors upon request. The sequences of the inserts were extensively verified using an ABI PRISM 3100-Avant Genetic Analyzer (Applied Biosystems). Recombinant baculoviruses were recovered using a BaculoGold transfection kit (Pharmingen) according to the manufacturer's instructions.

Antibodies. The mouse monoclonal antibodies (MAbs) used in this study were anti-hemagglutinin (anti-HA) MAb (12CA5; Roche), anti-FLAG (M2) MAb (Sigma), anti-c-*myc* MAb (9E10; Santa Cruz), anti-glyceraldehyde-3-phosphate dehydrogenase (anti-GAPDH) MAb (Chemicon), anti-GST MAb (Santa Cruz), anti-ubiquitin MAb (Chemicon), anti-E6AP MAb (E6AP-330) (Sigma), anticore MAb (B2; Anogen), and another anti-core MAb (2H9) (56). Polyclonal antibodies (PAbs) used in this study were anti-HA rabbit PAb (Y-11; Santa Cruz), anti-FLAG rabbit PAb (F7425; Sigma), anti-E6AP rabbit PAb (H-182; Santa Cruz), anti-DDX3 rabbit PAb (47), anti-PA28γ rabbit PAb (Affiniti), and anti-GST goat PAb (Amersham). Anticore rabbit PAb (TS1) was raised against the recombinant GST core protein.

MEF purification procedure. 293T cells were transfected with the plasmid expressing MEF core by the calcium phosphate precipitation method (4). After the cells were lysed, the expressed MEF core and its binding proteins were recovered following the procedure described previously (16). 293T cells transfected with pcDNA3-MEF core in four 10-cm dishes were lysed in 2 ml of lysis buffer: 50 mM Tris-HCl (pH 7.5), 150 mM NaCl, 10% (wt/vol) glycerol, 100 mM NaF, 1 mM Na_3VO_4, 1% (wt/vol) Triton X-100, 5 μM $ZnCl_2$, 2 mM phenylmethylsulfonyl fluoride, 10 μg/ml aprotinin, and 1 μg/ml leupeptin. The lysate was centrifuged at 100,000 × *g* for 20 min at 4°C. The supernatant was passed through a 5-μm filter, incubated with 100 μl of Sepharose beads for 60 min at 4°C, and then passed through a 0.65-μm filter. The filtered supernatant was mixed with 100 μl of anti-myc-conjugated Sepharose beads for the first immunoprecipitation. After incubation for 90 min at 4°C, the beads were washed five times with 1 ml of TNTG buffer (20 mM Tris-HCl, pH 7.5, 150 mM NaCl, 10% [wt/vol] glycerol, and 1% [wt/vol] Triton X-100), twice with 1 ml of buffer A (20 mM Tris-HCl, pH 7.5, 150 mM NaCl, and 1% [wt/vol] Triton X-100), and finally once with 1 ml of TNT buffer (50 mM Tris-HCl, pH 8.0, 150 mM NaCl, 1% [wt/vol] Triton X-100). The washed beads were incubated with 10 U of tobacco etch virus protease (Invitrogen) in TNT buffer (100 μl) to release bound protein complexes from the beads. After incubation for 60 min at room temperature, the supernatant was pooled and the beads were washed twice with 70 μl of buffer A. The resulting supernatants were combined and incubated with 12 μl of FLAG-Sepharose beads for the second immunoprecipitation. After incubation for 60 min at room temperature, the beads were washed three times with 240 μl of buffer A, and proteins bound to the immobilized HCV core protein on the FLAG beads were dissociated by incubation with 80 μg/ml FLAG peptide (NH_2-Asp-Tyr-Lys-Asp-Asp-Asp-Asp-Lys-COOH) (Sigma).

MS/MS. Proteins were separated by 9% sodium dodecyl sulfate-polyacrylamide gel electrophoresis (SDS-PAGE) and visualized by silver staining. The stained bands were excised and digested in the gel with lysylendoprotease-C (Lys-C), and the resulting peptide mixtures were analyzed using a direct nanoflow liquid chromatography-tandem mass spectrometry (MS/MS) system (33), equipped with an electrospray interface reversed-phase column, a nanoflow gradient device, a high-resolution Q-time of flight hybrid mass spectrometer (Q-TOF2; Micromass), and an automated data analysis system. All the MS/MS

spectra were searched against the nonredundant protein sequence database maintained at the National Center for Biotechnology Information using the Mascot program (Matrixscience) to identify proteins. The MS/MS signal assignments were also confirmed manually.

Expression and purification of recombinant proteins. *E. coli* BL21(DE3) cells were transformed with plasmids expressing GST fusion protein or His-tagged protein and grown at 37°C. Expression of the fusion protein was induced by 1 mM isopropyl-β-D-thiogalactopyranoside at 37°C for 4 h. Bacteria were harvested, suspended in lysis buffer (phosphate-buffered saline [PBS] containing 1% Triton X-100), and sonicated on ice.

Hi5 cells were infected with recombinant baculoviruses to produce GST-C173HT, GST-C152HT, GST-HT, MEF-E6AP, and His-tagged mouse E1 (17). GST and GST fusion proteins were purified on glutathione-Sepharose beads (Amersham Bioscience) according to the manufacturer's protocols. His-tagged proteins were purified on nickel-nitrilotriacetic acid beads (QIAGEN) according to the manufacturer's protocols. MEF-E6AP and MEF-E6AP C-A were purified on anti-FLAG M2 agarose beads (Sigma) according to the manufacturer's protocols.

Immunoblot analysis. Immunoblot analysis was performed essentially as described previously (11). The membrane was visualized with SuperSignal West Pico chemiluminescent substrate (Pierce).

HCV core protein and E6AP binding assays. To map the E6AP binding site on HCV core protein, 2.5 μg of purified recombinant GST-E6AP expressed in Hi5 cells was mixed with 1,000 μg of 293T cell lysates transfected with a series of FLAG-tagged HCV core deletion mutants as indicated. The protein concentration of the cells was determined using the bicinchoninic acid protein assay kit (Pierce). The mixtures were immunoprecipitated with anti-FLAG M2 agarose beads (Sigma), and proteins bound to the immobilized HCV core protein on anti-FLAG beads were dissociated with FLAG peptide (Sigma). The eluates were analyzed by immunoblotting with anti-GST PAb. To map the HCV core-binding site on E6AP, GST pull-down assays were performed as described previously (51).

In vivo ubiquitylation assay. In vivo ubiquitylation assays were performed essentially as described previously (57). FLAG-core was immunoprecipitated with anti-FLAG beads. Immunoprecipitates were analyzed by immunoblotting, using either anti-HA PAb or anticore PAb (TS1) to detect ubiquitylated core proteins.

In vitro ubiquitylation assay. For in vitro ubiquitylation of HCV core protein, purified GST-C173HT and GST-C152HT were used as substrates. Purified GST-HT was used as a negative control. Assays were done in 40-μl volumes containing 20 mM Tris-HCl, pH 7.6, 50 mM NaCl, 5 mM ATP, 10 mM $MgCl_2$, 8 μg of bovine ubiquitin (Sigma), 0.1 mM dithiothreitol, 200 ng mouse E1, 200 ng E2 (UbcH7), and 0.5 μg each of MEF-E6AP or MEF-E6AP C-A. The reaction mixtures were incubated at 37°C for 120 min followed by purification with glutathione-Sepharose beads and immunoblotting with the indicated antibodies.

siRNA transfection. 293T cells or Huh-7 cells at 3×10^5 cells in a six-well plate were transfected with 40 pmol of either E6AP-specific short interfering RNA (siRNA; Sigma) or scramble negative-control siRNA duplexes (Sigma) using HiPerFect transfection reagent (QIAGEN) following the manufacturer's instructions. The siRNA target sequences were as follows: E6AP (sense), 5′-GGGUC UACACCAGAUUGCUTT-3′; scramble negative control (sense), 5′-UUGCG GGUCUAAUCACCGATT-3′.

CHX half-life experiments. To examine the half-life of HCV core protein, transfected 293T cells were treated with 50 μg/ml cycloheximide (CHX) at 44 h posttransfection. The cells at zero time points were harvested immediately after treatment with CHX. Cells from subsequent time points were incubated in medium containing CHX at 37°C for 3, 6, and 9 h as indicated.

Infection of Huh-7 cells with secreted HCV. Infectious HCV JFH1 was produced in Huh-7.5.1 cells (61) as described previously (56). Culture supernatant containing infectious HCV JFH1 was collected and passed through a 0.22-μm filter. Naïve Huh-7 cells were seeded 24 h before infection at a density of 1×10^6 in a 10-cm dish. The cells were incubated with 2.5 ml of the inoculum (6.5×10^3 50% tissue culture infectious dose [$TCID_{50}$]/ml) for 3 h, washed three times with PBS, and supplemented with fresh complete Dulbecco's modified Eagle's medium. Then the cells were transfected with 6 μg each of pCAGGS, pCAG-HA-E6AP, or pCAG-HA-E6AP C-A by using TransIT LT1 (Mirus). The cells were trypsinized and replated in six-well plates at 1 day postinfection. The culture medium was changed every 2 days. The culture supernatants and the cells were collected at days 3 and 7 postinfection.

Quantitation of HCV RNA and core protein. We quantitated HCV core protein in cell lysate using the HCV core antigen enzyme-linked immunosorbent assay (ELISA) (Ortho-Clinical Diagnostics). Total RNA was extracted from cells using TRIzol reagent (Invitrogen). To quantitate HCV RNAs, real-time reverse transcription-PCR was performed as described previously (53).

Infectivity assay. The $TCID_{50}$ was calculated essentially based on the method described previously (28). Virus titration was performed by seeding Huh-7 cells in 96-well plates at 1×10^4 cells/well. Samples were serially diluted fivefold in complete growth medium and used to infect the seeded cells (six wells per dilution). Following 3 days of incubation, the cells were immunostained for core with anticore MAb (2H9). Wells that expressed at least one core-expressing cell were counted as positive, and the $TCID_{50}$ was calculated.

Immunocytochemistry and fluorescence microscopy. Cells on collagen-coated coverslips were washed with PBS, fixed with 4% paraformaldehyde for 30 min at 4°C, and permeabilized with PBS containing 0.2% Triton X-100. Cells were preincubated with BlockAce (Dainippon Pharmaceuticals), incubated with specific antibodies as primary antibodies, washed, and incubated with rhodamine-conjugated goat anti-rabbit immunoglobulin G (ICN Pharmaceuticals, Inc.) and Qdot 565-conjugated goat anti-mouse immunoglobulin G (Quantumdot) as secondary antibody. Then the cells were washed with PBS, counterstained with DAPI (4′,6′-diamidino-2-phenylindole) solution (Sigma) for 3 min, mounted on glass slides, and examined with a BZ-8000 microscope (Keyence).

Knockdown of endogenous E6AP in HCV JFH1-infected Huh-7 cells. Naïve Huh-7 cells at 10^6 cells/10-cm dish were inoculated with 2.5 ml of the inoculum including infectious HCV JFH1 (6.5×10^3 $TCID_{50}$/ml) and cultured. The cells were replated in a six-well plate at 3×10^5 cells/well at day 11 postinfection and transfected with 40 pmol of E6AP siRNA or control siRNA. The culture medium was changed at 24 h after transfection. The cells were harvested at day 2 after transfection, and the intracellular core protein levels were quantitated using the HCV core antigen ELISA. The culture supernatants were collected at day 2 after transfection and assayed for $TCID_{50}$ determinations.

RESULTS

Identification of E6AP as an HCV core-binding protein. To identify the molecular machinery for HCV core ubiquitylation, we searched for endogenous ubiquitin-proteasome pathway proteins that associated with HCV core protein. HCV core-binding proteins (i.e., MEF core and its binding proteins, recovered from lysed cells) were purified by a tandem affinity purification procedure using a tandem tag (known as MEF tag) (16). Ten proteins were reproducibly detected (Fig. 1A, lane 2), but none were recovered from lysed control cells transfected with empty vector alone (Fig. 1A, lane 1).

To identify the proteins, silver-stained bands were excised from the gel, digested by Lys-C, and analyzed using a direct nanoflow liquid chromatography-MS/MS system. Nine proteins were identified: two known HCV core-binding proteins, human DEAD box protein DDX3 (38) and proteasome activator PA28-γ (30), and seven potential HCV core-binding proteins. E6AP was identified (Fig. 1A, lane 2) on the basis of five independent MS/MS spectra (Table 1). Immunoblot analyses confirmed the proteomic identification of E6AP, DDX3, PA28-γ, and MEF-core (Fig. 1B to E).

E6AP binding domain for HCV core protein. The E6AP binding domain for HCV core protein was investigated. Figure 2A is a schematic representation of E6AP and known motifs in E6AP. A series of deletion mutants of E6AP as GST fusion proteins were expressed in *E. coli*. GST pull-down assays found that the carboxyl-terminal deletion mutant E6AP (1–517), but not E6AP (1–418) (Fig. 2C, lanes C and D), and the amino-terminal deletion mutant E6AP (418–875), but not E6AP (517–875) (Fig. 2C, lanes J and K), were able to bind to the core protein. The signal was absent when unprogrammed wheat germ extracts (the negative control) were used as a source of proteins (data not shown). GST pull-down assays (Fig. 2B) found that the region from aa 418 to aa 517 is important for binding to the HCV core protein. An assay of the

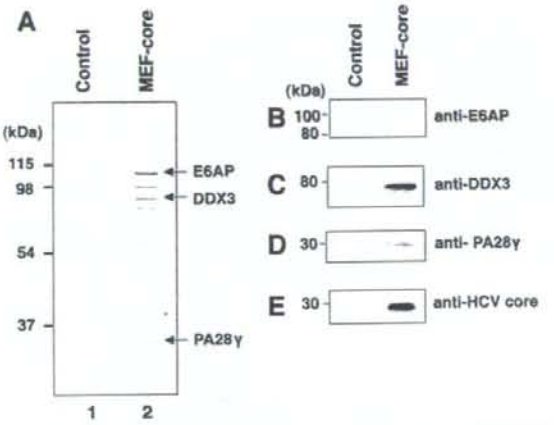

FIG. 1. HCV core protein associates with E6AP in vivo. (A) 293T cells were transfected with pcDNA3-MEF-core or empty plasmid, incubated for 48 h, and then harvested. The expressed MEF-core and binding proteins were recovered using the MEF purification procedure. Proteins bound to the MEF-core immobilized on anti-FLAG beads were dissociated with FLAG peptides, resolved by 9% SDS-PAGE, and visualized by silver staining. Control experiments were performed using 293T cells transfected with vector alone. The positions of E6AP, DDX3, and PA28γ are indicated by arrows. (B to E) The proteins detected in panel A were confirmed by immunoblotting with appropriate antibodies: E6AP (B), DDX3 (C), PA28γ (D), and MEF-core (E).

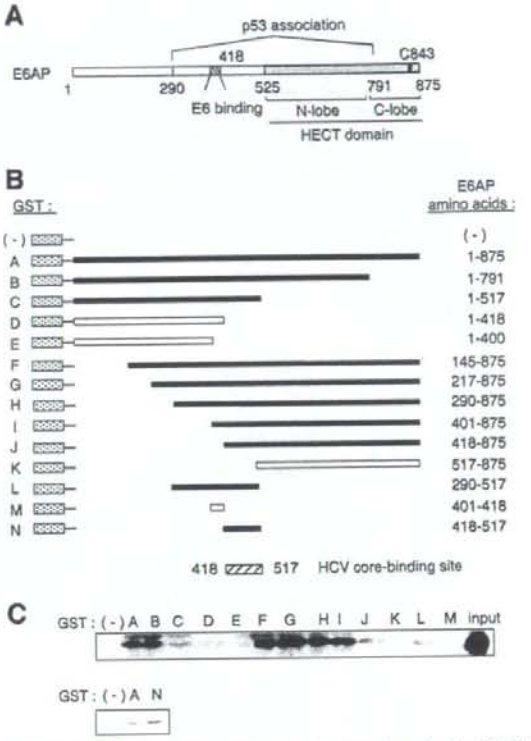

FIG. 2. Mapping of the HCV core-binding domain for E6AP. (A) Structure of E6AP. Shown is a schematic representation of the regions of E6AP isoform II that mediate E6 binding (aa 401 to 418), E6-dependent association with p53 (aa 290 to 791), and the HECT catalytic domain (aa 525 to 875). The catalytic cysteine residue is located at aa 843. (B) Schematic representation of GST-E6AP proteins. GST proteins A through N contain the E6AP amino acids indicated to the right. The shaded region of each represents the GST sequence. Closed boxes represent proteins that are bound specifically to HCV core protein, and open boxes represent those that are not bound. (C) Binding of HCV core protein to GST-E6AP proteins A through N. In vitro-translated core protein (aa 1 to 173) was assayed for association with GST (-) or the GST-E6AP fusion proteins A through N. Association of core protein was detected by immunoblotting with anti-core MAb.

ability of GST-E6AP (418–517) to bind to the HCV core protein was confirmatory (Fig. 2C, lane N) and led to the conclusion that the HCV core-binding domain of E6AP was aa 418 to aa 517.

The HCV core-binding domain for E6AP. By use of a panel of HCV core deletion mutants (Fig. 3A), GST-E6AP was found to coimmunoprecipitate with all of the FLAG-core proteins (Fig. 3A, lanes A to H) except FLAG-core (72–191) or FLAG-core (92–191) (Fig. 3A, lanes I and J). No association of control GST protein with any FLAG-core proteins was observed (data not shown). These data suggest that the aa-58-to-aa-71 segment of the HCV core binds to E6AP. The ability of GST-core (58–71) to associate with purified MEF-E6AP confirmed that the core (aa 58–71) was the site for E6AP binding on the HCV core protein (Fig. 3B).

E6AP decreases steady-state levels of HCV core protein in 293T cells and HepG2 cells. One of the features of HECT domain ubiquitin ligases is direct association with their substrates (50). Thus, we hypothesized that E6AP would function as an E3 ubiquitin ligase for the HCV core protein. We assessed the effects of E6AP on the HCV core protein in 293T cells. FLAG-core (1–191) together with HA-tagged wild-type E6AP, catalytically inactive mutant E6AP, E6AP C-A (19), or WWP1 (another HECT domain ubiquitin ligase) (22) was introduced into 293T cells, and the levels of the core protein were examined by immunoblotting. The steady-state levels of the core protein decreased with an increase in the amount of E6AP plasmids (Fig. 4A and B). However, neither E6AP C-A mutant nor WWP1 decreased the steady-state levels of the core protein, suggesting that E6AP enhances degradation of the core protein.

To verify the critical need for endogenous E6AP in the core degradation, expression of E6AP was knocked down by siRNA and the expression of the core protein and E6AP was assayed by immunoblotting. Transfection of the E6AP-specific siRNA

TABLE 1. Identification of E6AP by tandem mass spectrometry[a]

Peptide *m/z*	Sequence determined	Residues
720.9	VFSSAEALVQSFR	156–168
922.4	AACSAAAMEEDSEASSSR	196–213
774.9	MMETFQQLITYK	339–350
1,053.1	ITVLYSLVQGQQLNPYLR	507–524
809.4	EFVISYSDYILNK	712–724

[a] The protein was ubiquitin protein ligase E3A (E6AP) isoform 2 (GenBank accession no. NP_000453).

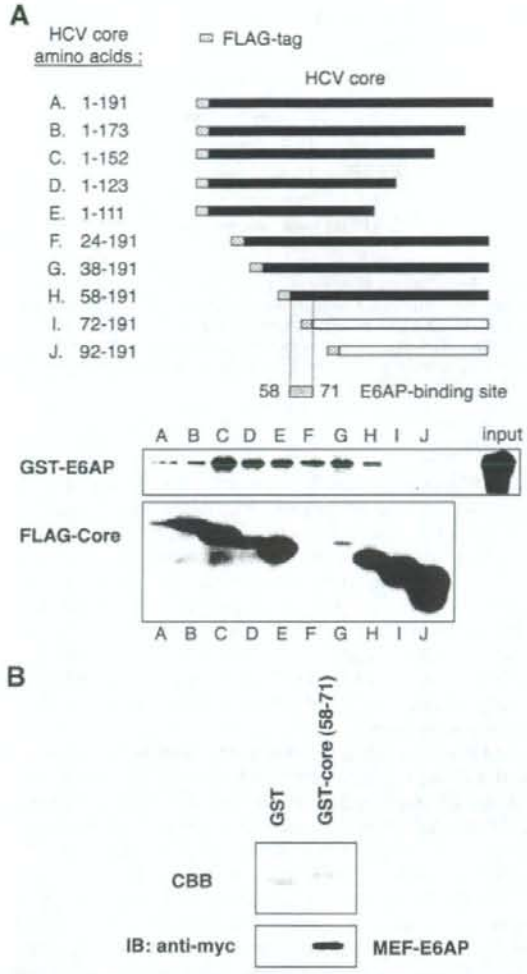

FIG. 3. Mapping of the E6AP binding domain for HCV core protein. (A) In vitro binding of E6AP to HCV core protein. 293T cells were transfected with each plasmid indicated in the upper panel. At 48 h posttransfection, cell lysates were mixed with purified GST-E6AP, immunoprecipitated with anti-FLAG beads, and then immunoblotted with anti-GST PAb (middle panel) or anti-FLAG MAb (bottom panel). The last lane (input) represents GST-E6AP used in this assay (middle panel). (B) Binding of GST-core (aa 58 to aa 71) to purified MEF-E6AP. GST served as a negative control for binding. Upper panel, Coomassie blue-stained SDS-PAGE of GST and GST-core (58–71). Lower panel, results of the GST pull-down assay. MEF-E6AP was detected by anti-myc MAb. CBB, Coomassie brilliant blue; IB, immunoblot.

duplex reduced the protein level of E6AP by 90% at 48 h posttransfection (Fig. 4C, middle panel). Immunoblotting revealed a 4.1-fold increase in the level of the core protein in the cells transfected with E6AP siRNA (Fig. 4C, top panel), suggesting that endogenous E6AP plays a role in the proteolysis of the HCV core protein.

Then we examined whether E6AP reduces the steady-state

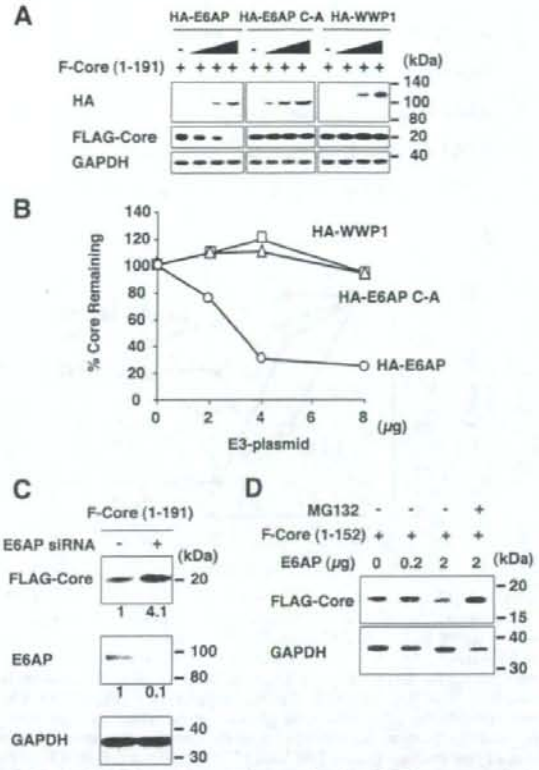

FIG. 4. E6AP decreases steady-state levels of HCV core protein in 293T cells and in HepG2 cells. (A) 293T cells (1×10^6 cells/10-cm dish) were transfected with 1 μg of pCAG FLAG-core (1–191) along with either pCAG-HA-E6AP, pCAG-HA-E6AP C-A, or pCAG-HA-WWP1 as indicated. At 48 h posttransfection, protein extracts were separated by SDS-PAGE and analyzed by immunoblotting with anti-HA PAb (top panel), anti-FLAG MAb (middle panel), and anti-GAPDH MAb (bottom panel). (B) Quantitation of data shown in panel A. Intensities of the gel bands were quantitated using the NIH Image 1.62 program. The level of GAPDH served as a loading control. Circles, E6AP; triangles, E6AP C-A; squares, WWP1. (C) Knockdown of endogenous E6AP by siRNA inhibits degradation of HCV core protein in 293T cells. 293T cells (3×10^5 cells/six-well plate) were transfected with 40 pmol of E6AP-specific duplex siRNA (or control siRNA) as described in Materials and Methods. The cells were transfected with 2 μg of FLAG-core (1–191) expression plasmid and cultured for 24 h, harvested, and analyzed by immunoblotting. Shown is immunoblot detection of FLAG-tagged core protein (top panel), E6AP protein (middle panel), and GAPDH (bottom panel) in control siRNA-treated 293T cells or E6AP-siRNA-treated 293T cells. The relative levels of protein expression were quantitated by densitometry and indicated below in the respective lanes. GAPDH served as a loading control. (D) HepG2 cells (2×10^5 cells/six-well plate) were transfected with pCAG FLAG-core (1–152) along with either empty vector or pCMV E6AP as indicated. The cells were harvested at 44 h posttransfection. Where indicated, cells were treated with 25 μM MG132 or with dimethyl sulfoxide control 14 h prior to collection. Equivalent amounts of the whole-cell lysates were separated by SDS-PAGE and analyzed by immunoblotting with anti-FLAG MAb (upper panel) or anti-GAPDH MAb (lower panel).

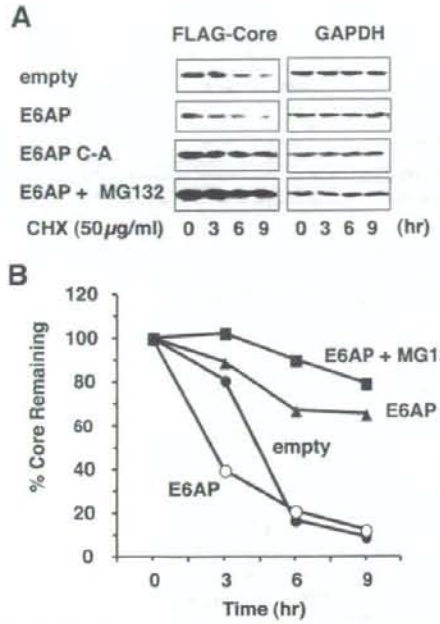

FIG. 5. Kinetic analysis of E6AP-dependent degradation of HCV core protein. (A) 293T cells (1×10^6 cells/10-cm dish) were transfected with 1 μg of pCAG-FLAG core (1–152) plus 4 μg of empty vector, pCMV-HA-E6AP, or pCMV-HA-E6AP C-A. The cells were treated with 50 μg/ml CHX at 44 h after transfection. Cell extracts were collected at 0, 3, 6, and 9 h after treatment with CHX, followed by immunoblotting. (B) Specific signals were quantitated by densitometry, and the percent remaining core at each time was compared with that at the starting point. The level of GAPDH served as a loading control. Open circles, E6AP; closed circles, empty plasmid; closed triangles, E6AP C-A; closed squares, E6AP with MG132 treatment. Data are representative of three independent experimental determinations.

levels of the core protein in hepatic cells as well as in 293T cells. Exogenous expression of E6AP resulted in reduction of the core protein in human hepatoblastoma HepG2 cells (Fig. 4D). Treatment of the cells with the proteasome inhibitor MG132 increased the core protein level, suggesting that the core protein was degraded through the ubiquitin-proteasome pathway. These results indicate that E6AP enhances proteasomal degradation of the HCV core protein in both hepatic cells and nonhepatic cells.

Kinetic analysis of E6AP-dependent degradation of HCV core protein. To determine whether the E6AP-induced reduction of the core protein is due to an increase in the rate of core degradation, we performed kinetic analysis using the protein synthesis inhibitor CHX. HCV core protein together with wild-type E6AP or inactive mutant E6AP C-A was expressed in 293T cells. At 44 h after transfection, cells were treated with either 50 μg/ml CHX alone or 50 μg/ml CHX plus 25 μM MG132 to inhibit proteasome function. Cells were collected at 0, 3, 6, and 9 h following treatment and analyzed by immunoblotting (Fig. 5A). Overexpression of E6AP resulted in rapid degradation of the core protein, whereas inactive mutant

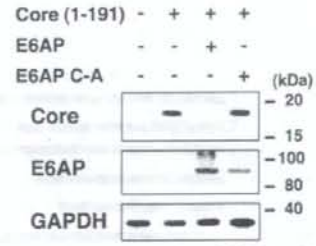

FIG. 6. E6AP promotes degradation of full-length HCV core protein in Huh-7 cells. Huh-7 cells (2×10^5 cells/six-well plate) were transfected with 0.5 μg of pCAG-core (1–191) together with 2 μg of pCMV-HA-E6AP or pCMV-HA-E6AP C-A. At 48 h posttransfection, cells were harvested and analyzed by immunoblotting with anticore MAb (top panel), anti-E6AP PAb (middle panel), or anti-GAPDH MAb (bottom panel).

E6AP C-A increased the half-life of the core protein (Fig. 5B), suggesting that the inactive E6AP inhibited degradation of the core protein in a dominant-negative manner, which is in agreement with previous studies (19, 55). Treatment of the cells with MG132 inhibited the degradation of the core protein (Fig. 5B). Reverse transcription-PCR to determine mRNA levels of the HCV core gene and GAPDH gene found that neither wild-type E6AP nor inactive E6AP changed mRNA levels of the HCV core gene and GAPDH gene (data not shown). These results indicate that E6AP enhances proteasomal degradation of the core protein.

E6AP promotes degradation of the full-length core protein in Huh-7 cells. To determine whether the full-length HCV core protein expressed in hepatic cells is degraded through an E6AP-dependent pathway, human hepatoma Huh-7 cells were transfected with pCAG HCV core (1–191) along with either E6AP or E6AP C-A. To rule out the effects of N-terminal FLAG tag on the core degradation, HCV core protein was expressed as untagged protein. Expression of wild-type E6AP resulted in reduction of the core protein (Fig. 6). On the other hand, HCV core protein was not decreased after transfection of inactive E6AP, indicating that the full-length core protein expressed in Huh-7 cells is also degraded through an E6AP-dependent pathway.

E6AP mediates ubiquitylation of HCV core protein in vivo. To determine whether E6AP can induce ubiquitylation of HCV core protein in cells, we performed in vivo ubiquitylation assays. 293T cells were cotransfected with FLAG-core (1–191) and either E6AP or empty plasmid, together with a plasmid encoding HA-tagged ubiquitin to facilitate detection of ubiquitylated core protein. Cell lysates were immunoprecipitated with anti-FLAG MAb and immunoblotted with anti-HA PAb to detect ubiquitylated core protein (Fig. 7A). Only a little ubiquitin signal was observed on the core protein in the absence of cotransfected E6AP (Fig. 7A, lane 3). In contrast, coexpression of E6AP led to readily detectable ubiquitylated forms of the core protein as a ladder and a smear of higher-molecular-weight bands (Fig. 7A, compare lane 3 with lane 4). Immunoblot analysis with anticore PAb confirmed that FLAG-core proteins were immunoprecipitated (Fig. 7B, lanes 2 to 4, short exposure) and that higher-molecular-weight bands con-